

## Transportation Science

Publication details, including instructions for authors and subscription information:  
<http://pubsonline.informs.org>

### A Stochastic Optimization Model for Designing Last Mile Relief Networks

Nilay Noyan, Burcu Balcik, Semih Atakan

To cite this article:

Nilay Noyan, Burcu Balcik, Semih Atakan (2016) A Stochastic Optimization Model for Designing Last Mile Relief Networks. *Transportation Science* 50(3):1092-1113. <https://doi.org/10.1287/trsc.2015.0621>

Full terms and conditions of use: <https://pubsonline.informs.org/page/terms-and-conditions>

This article may be used only for the purposes of research, teaching, and/or private study. Commercial use or systematic downloading (by robots or other automatic processes) is prohibited without explicit Publisher approval, unless otherwise noted. For more information, contact permissions@informs.org.

The Publisher does not warrant or guarantee the article's accuracy, completeness, merchantability, fitness for a particular purpose, or non-infringement. Descriptions of, or references to, products or publications, or inclusion of an advertisement in this article, neither constitutes nor implies a guarantee, endorsement, or support of claims made of that product, publication, or service.

Copyright © 2015, INFORMS

Please scroll down for article—it is on subsequent pages

INFORMS is the largest professional society in the world for professionals in the fields of operations research, management science, and analytics.

For more information on INFORMS, its publications, membership, or meetings visit <http://www.informs.org>



# A Stochastic Optimization Model for Designing Last Mile Relief Networks

Nilay Noyan

Industrial Engineering Program, Sabancı University, 34956 Istanbul, Turkey, [nnoyan@sabanciuniv.edu](mailto:nnoyan@sabanciuniv.edu)

Burcu Balcik

Industrial Engineering Department, Özyegin University, 34794 Istanbul, Turkey, [burcu.balcik@ozyegin.edu.tr](mailto:burcu.balcik@ozyegin.edu.tr)

Semih Atakan

Industrial Engineering Program, Sabancı University, 34956 Istanbul, Turkey, [semihatakan@sabanciuniv.edu](mailto:semihatakan@sabanciuniv.edu)

In this study, we introduce a distribution network design problem that determines the locations and capacities of the relief distribution points in the last mile network, while considering demand- and network-related uncertainties in the post-disaster environment. The problem addresses the critical concerns of relief organizations in designing last mile networks, which are providing accessible and equitable service to beneficiaries. We focus on two types of supply allocation policies and propose a hybrid version considering their different implications on equity and accessibility. Then, we develop a two-stage stochastic programming model that incorporates the hybrid allocation policy and achieves high levels of accessibility and equity simultaneously. We devise a branch-and-cut algorithm based on Benders decomposition to solve large problem instances in reasonable times and conduct a numerical study to demonstrate the computational effectiveness of the solution method. We also illustrate the application of our model on a case study based on real-world data from the 2011 Van earthquake in Turkey.

**Keywords:** distribution network design; post-disaster; humanitarian relief; accessibility; equity; stochastic integer programming; L-shaped method; branch-and-cut

**History:** Received: November 2013; revisions received: October 2014, February 2015; accepted: March 2015.  
Published online in *Articles in Advance* August 10, 2015.

## 1. Introduction

A severe earthquake hit the city of Van in Turkey on October 23rd, 2011, damaging most of the residential units in the city and leaving thousands of people in immediate need of basic relief supplies (such as shelter, food, and clothing). The earthquake also damaged the local airport and infrastructure (IFRC 2012). Despite the immediate response of local relief organizations and a large amount of donations collected, there were challenges in meeting the needs. According to local news and agency reports (see Avci 2011; Ziflioğlu 2011), a systematic aid delivery system could not be established in the area and there was an uneven distribution of relief supplies among the population. Moreover, it was reported that some people could not access aid as they had to walk long distances to reach the relief distribution points. As also observed during other disaster relief operations (e.g., the 2005 Pakistan earthquake, 2010 Haiti earthquake), organizations may face serious logistical challenges in the “*last mile*”; such challenges include (i) the unpredictable and chaotic environment, (ii) the high stakes associated with quick demand satisfaction, (iii) the

damaged transportation infrastructure, and (iv) the scarcity of resources (Kovacs and Spens 2007; Balcik et al. 2008). Given these challenges, it is critical for relief organizations to establish last mile networks that would allow the affected people to access relief supplies in an effective and equitable way.

An example of a last mile network is illustrated in Figure 1. As shown in the figure, relief supplies arriving at a local distribution center (LDC) are sent to points of distribution (PODs), where beneficiaries are delivered relief supplies. LDCs are large warehouses that store and distribute supplies to the PODs. Depending on the situation, each POD can serve one or several demand locations (such as neighborhoods, villages, or camps) scattered over the affected area. In last mile networks, it is typical that people in the affected regions travel (or walk) to the PODs to receive relief supplies. In some cases, vehicles might transport supplies from PODs to beneficiaries. In both situations, it is crucial to consider the factors that can affect access to aid.

Last mile relief networks are usually set up temporarily based on the initial assessments of the

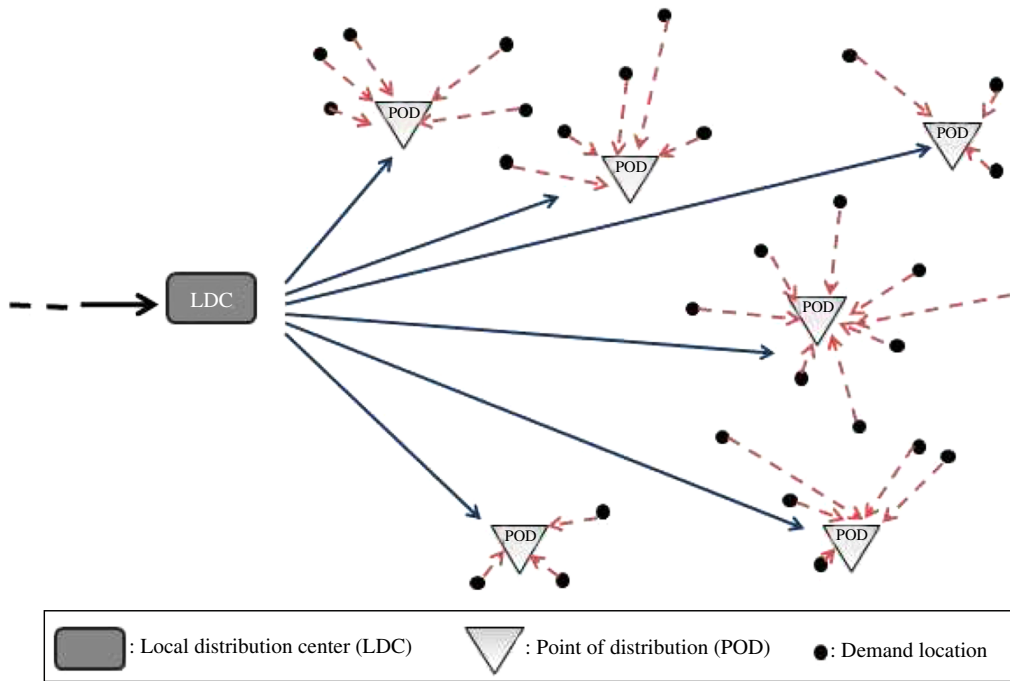


**Figure 1** (Color online) Example of Last Mile Relief Network

Source. Modified from Horner and Downs (2007)

relief organizations about the post-disaster conditions and needs. However, available information at this stage are usually rough and incomplete. Therefore, to immediately start delivering the relief supplies to the affected areas, the relief organizations need to determine the locations and capacities of the PODs under significant uncertainty. Given that last mile relief network design decisions can significantly affect the performance of disaster response (in terms of response time, accessibility, equity, etc.), it is important to develop decision-making models that effectively incorporate the uncertain aspects of the post-disaster environment.

In this paper, we study the stochastic last mile relief network design problem (SLMRND), which determines the locations and capacities of PODs to be located in the last mile network, assigns demand locations to the PODs, and allocates available supplies among the PODs while considering the *uncertainty* in post-disaster relief demands and transportation network conditions. We consider a single LDC, whose location is fixed and known. SLMRND incorporates the important characteristics of the last mile environment, which, to the best of our knowledge, have not been considered in a stochastic setting before. Specifically, we characterize (i) *accessibility* and (ii) *equity* in the context of last mile relief network design, and develop metrics to incorporate these critical concerns into optimization models.

Ensuring a high level of *accessibility* in the last mile network is an important goal while locating PODs.

As stressed by the Sphere Standards ([Sphere Project 2011](#), p. 194), "distribution points should be established where they are safe and most convenient for the recipients, not based on logistic convenience for the [distributing] agency." Locating the last mile facilities solely based on pre-disaster network travel times may not ensure accessibility. Indeed, post-disaster network conditions and characteristics (such as damaged roads and topographical barriers) can strongly affect accessibility. Also, demographic (such as gender and age) and socioeconomic (such as vehicle ownership) characteristics of the affected population groups must be taken into account, as these factors can have a significant impact on the mobility of people, and hence on their access to relief supplies. Another critical consideration in last mile relief network design is ensuring *equity*. As also highlighted by Sphere Standards ([Sphere Project 2011](#), p. 310), humanitarian services must be provided according to "the principles of equity and impartiality, ensuring equal access according to need without any discrimination." The locations and capacities of PODs in the last mile network can significantly affect the ease of access to the relief supplies by different population groups as well as the amount of supplies allocated to each population group.

In this paper, we characterize the concepts of accessibility and equity in the context of last mile relief network design, and develop performance metrics to incorporate these important concerns into models. We focus on two supply allocation policies to equitably

distribute the available relief supplies among the selected PODs and show that there can be significant differences between the performance of these policies in terms of accessibility and equity. Considering their different benefits, we propose a hybrid allocation policy and develop a two-stage stochastic programming model that incorporates this hybrid policy and can achieve high levels of equity and accessibility simultaneously. In our stochastic optimization model, we capture the uncertainty in post-disaster demands and transportation network conditions through a finite set of scenarios. We also construct a case study based on the real-world data from the 2011 Van earthquake in Turkey and perform numerical analysis to illustrate the performance of the model. Because solving the proposed stochastic programming model is computationally challenging for the large instances of SLMRND, we develop an effective branch-and-cut algorithm based on Benders decomposition. We conduct a comprehensive numerical study that demonstrates the computational effectiveness of the solution method.

The rest of the paper is organized as follows. We review the relevant literature in §2. Section 3 describes the problem in detail. Section 4 presents the mathematical programming model and discusses its analytical characteristics. The solution method follows in §5. Section 6 presents a case study and an extensive numerical analysis. Finally, we discuss future research and conclude the paper in §7.

## 2. Literature Review

In this section, we review the relevant literature on post-disaster network design problems (§2.1) and stochastic programming algorithms (§2.2).

### 2.1. Post-disaster Network Design in Humanitarian Relief

Most studies related to post-disaster humanitarian operations focus on last mile distribution problems addressing vehicle routing and/or supply allocation decisions (e.g., Barbarosoglu and Arda 2004; Tzeng et al. 2007; Balcik et al. 2008; Huang, Smilowitz, and Balcik 2012). Only a few studies address the problem of designing last mile networks. Horner and Downs (2008) consider locating distribution points in a hurricane region for providing relief supplies after the disaster. The authors present an integer programming model that determines the locations of PODs, the assignments of PODs to LDCs, and the assignments of the demand locations to PODs, minimizing the total cost of distributing the relief goods. They test the model on real-world data and stress the consideration of socioeconomic factors (i.e., household income levels) in locating distribution points. The model presented in Horner and Downs (2008) is extended by

Horner and Downs (2010) and Widener and Horner (2011). Horner and Downs (2010) include the decisions on the amount of goods delivered from the LDCs to the PODs, and Widener and Horner (2011) consider multiple types of distribution points, where each type of facility can offer different relief goods and services. Horner and Widener (2011) consider a capacitated  $p$ -median model to locate post-hurricane facilities and simulate the model in an uncertain environment to investigate the effects of link failures on the location decisions. Some studies consider location and transportation decisions simultaneously in a post-disaster setting (e.g., Yi and Ozdamar 2007; Rath and Gutjahr 2011; Afshar and Haghani 2012; Lin et al. 2012; Tricoire, Graf, and Gutjahr 2012). The majority of these studies involving post-disaster network design decisions either assume a deterministic setting and/or do not incorporate accessibility and equity.

A multitude of factors affecting accessibility in the last mile have been discussed in the literature. For instance, IFRC (2013) and OCHA (2013) discuss the effects of damaged transportation infrastructure on accessibility during relief efforts after the floods in Ghana and Sudan, respectively. Stephenson (1993) describes the challenging effects of topographic factors on Ethiopian drought/famine relief in 1984–1985. There are also studies (e.g., Morrow 1999; Kovacs and Tatham 2009; Zakour and Harrell 2004) that stress the importance of demographic/socioeconomic factors (such as race, age, gender, income level, being in a female-headed household with young children) on access to aid. The literature lacks studies that present metrics/objectives that incorporate such accessibility-related factors in designing last mile relief networks.

Equity has been considered as an important issue in the humanitarian logistics literature (e.g., Tzeng et al. 2007; Balcik et al. 2008; Vitoriano et al. 2011). A common approach for modeling equity is to focus on the worst value of a performance metric of interest (such as the maximum distance between facilities and users in the  $p$ -center model) and optimize or bound the worst value through the objective function or the constraints, respectively. Some studies analyze the trade-offs between using equity- and efficiency-related objectives in different disaster/emergency contexts (e.g., Felder and Brinkmann 2002; Campbell et al. 2008; Huang, Smilowitz, and Balcik 2012); specifically, they evaluate the impact of improving equity on various efficiency metrics (such as the total distance or cost). Although equity is considered as an important criterion in locating facilities in other settings (such as locating public facilities including fire/ambulance stations and libraries, e.g., Mulligan 1991; Marsh and Schilling 1994; Noyan 2010), equity in last mile relief network design has not been studied in detail.

This paper contributes to the humanitarian relief literature by characterizing the concepts of accessibility and equity within the context of last mile distribution network design, developing performance metrics, and presenting a mathematical model that incorporates accessibility and equity and at the same time captures the uncertain aspects of the post-disaster environment.

## 2.2. Stochastic Programming Algorithms

Stochastic programming models are generally known to be computationally challenging, which can partially be attributed to the potentially large number of scenario-dependent variables and constraints. Various decomposition-based solution methods have been proposed for two-stage stochastic programs. The (continuous) *L*-shaped method proposed by [Van Slyke and Wets \(1969\)](#) is a widely applied Benders decomposition approach to solve two-stage stochastic linear programming problems with the expected second-stage objective functions for the case of a finite probability space. This decomposition method and its variants (e.g., [Ahmed 2006; Noyan 2012](#)) are based on the duality theory of linear programming, and therefore cannot be applied to the two-stage linear problems with integer variables in the second stage.

Introducing integer variables into stochastic programs brings further complications; see [Birge and Louveaux \(1997\)](#), [Klein Haneveld and van der Vlerk \(1999\)](#), and [Sen \(2005\)](#) for a detailed discussion on solving stochastic integer programming models. To deal with stochastic programs with integer variables in both stages, [Laporte and Louveaux \(1993\)](#) propose the integer *L*-shaped algorithm, which is based on Benders decomposition. It utilizes a branch-and-cut scheme in the master problem and requires pure binary first stage decision variables. [Sen and Higle \(2005\)](#) and [Yuan and Sen \(2009\)](#) consider a special case of this setting with binary variables in the first-stage and mixed-binary variables in the second stage. The authors develop disjunctive decomposition-based branch-and-cut algorithms, which are in general computationally very effective (e.g., [Ntiamo and Sen 2008](#)). However, they assume that the recourse matrix<sup>1</sup> of the second-stage problem is deterministic. By contrast, in our models all of the second-stage parameters (including the recourse matrix, cost coefficients, and right-hand sides) can be random; specifically, the recourse matrix is scenario dependent because of the stochastic coverage sets and total demands at the POD level. In addition, the integer *L*-shaped method appears to be more easy to

implement than the disjunctive decomposition-based branch-and-cut algorithms.

One of the key contributions of this paper is developing a computationally effective solution algorithm that exploits the special structure of the proposed two-stage stochastic programming model. In particular, we implement an enhanced version of the classical integer *L*-shaped method ([Laporte and Louveaux 1993](#)) by employing state-of-the-art computational features, such as the lazy constraint callback of CPLEX, which proves useful to remove the burden of implementing a full-fledged branch-and-cut algorithm procedure ([Rubin 2011](#)). As emphasized in [Sen and Bulbul \(2015\)](#), the lazy constraint callback feature has been rarely used in operations research literature. To the best of our knowledge, devising such an enhanced integer *L*-shaped method is a first in the literature.

## 3. Problem Description

Given a network that involves a set of demand locations, a set of candidate PODs, and a single LDC (as in Figure 1), SLMRND determines (i) the locations and capacities of the PODs, (ii) the amounts of supplies to be delivered from the LDC to PODs, and (iii) the assignments of the demand points to the PODs, while considering equity and accessibility issues and incorporating demand and transportation network uncertainties. We describe the characteristics of SLMRND in the following subsections.

### 3.1. Network Structure and Facilities

The number and type of facilities in last mile networks may depend on various factors, such as the size of the relief organization or the scale of the operations. However, typically there are one or a few LDCs, each serving a fixed area through several PODs. For instance, after the Van earthquake, relief supplies were first accepted by a reception center close to the airport, and then shipped to the facilities in the last mile. Similarly, SLMRND assumes a single LDC, whose location is predetermined, and focuses on determining the locations and capacities of the PODs. Although the candidate PODs (such as schools, sports halls, or prefabricated structures) can exist anywhere on the network, we assume, without loss of generality, that the candidate POD set is a subset of the demand location set.

In SLMRND, each demand location is served by a single POD. Single sourcing is common in practice as it allows one to register beneficiaries and track whether the aid reaches those intended effectively. We assume an upper limit on the number of PODs, which can be determined based on available budget and human resources. The capacity of each POD depends on the demand assignments, which will be

<sup>1</sup> Recourse matrix represents the coefficients associated with the second-stage (recourse) decisions in the constraints of the second-stage problem. For example, see (23), where  $W^s$  represents the recourse matrix associated with scenario  $s$ .

determined in the model endogenously. However, we impose a maximum capacity limit for each POD to prevent oversized facilities.

### 3.2. Demand and Transportation Network Uncertainties

Although people may need different types of supplies (e.g., tents, blankets, food) after a disaster, relief organizations usually bundle different supplies into standard kits/pallets. Therefore, we consider a single type of relief item in SLMRND. The exact needs of the affected population are not immediately known and can only be estimated roughly at the time of designing the last mile relief network. In SLMRND, we represent demand uncertainty by a finite set of scenarios. In the Van earthquake case study (§6), we describe an approach to construct the demand scenarios using the available real-world data including population, earthquake strength, and distance to the epicenter.

As in the Van earthquake, disasters can damage the transportation network and reduce the capacity of some links (e.g., roads and bridges). There is usually a high level of uncertainty in the transportation network while making the post-disaster network design decisions. In SLMRND, the randomness in post-disaster link capacities is also characterized through a finite set of scenarios.

### 3.3. Performance Metrics

In this section, we characterize accessibility and equity, and develop performance metrics to incorporate these important concerns into the models for SLMRND.

**3.3.1. Accessibility.** In this study, we define accessibility as the *ease of access to the PODs/relief supplies*. To develop accessibility metrics, we focus on the two echelons of the last mile relief network separately; specifically, we consider: (i) accessibility of the PODs from the LDC, and (ii) accessibility of the PODs from the demand locations (see Figure 1). Vehicles carry supplies from the LDC to PODs in the first echelon, and people at demand locations travel/walk to PODs to receive supplies in the second echelon.

The concept of accessibility in a post-disaster setting is closely related to the response time. However, characterizing and measuring accessibility solely based on travel distances or pre-disaster travel times is not sufficient in the last mile network. For instance, in the Van earthquake relief, considering the possibility of damaged infrastructure (i.e., flooded and damaged roads) would have been essential. In addition, since the Van earthquake hit an underdeveloped region, it would also have been important to consider socially disadvantaged populations (e.g., individuals with low mobility such as the elderly, disabled, and women with small children) while characterizing and

measuring accessibility. In general, we classify the factors that may affect accessibility as (i) the physical factors (e.g., geographical, topographical, infrastructural) that affect post-disaster transportation times, and (ii) the demographic/socioeconomic factors (e.g., age, gender, economic status) that affect the mobility of individuals. Consequently, we assume that accessibility along the first echelon of the last mile network is affected only by the physical factors, whereas accessibility in the second echelon is affected both by physical factors and demographic/socioeconomic factors. Quantifying the effects of the latter on accessibility can especially be challenging. In this study, we develop an approach that computes an accessibility score for each link by adjusting the post-disaster travel times based on the proportion of the population with low mobility at the demand nodes (see §6 for details).

The main accessibility metric we consider in modeling SLMRND is the *expected total accessibility (ETA)*, which is the sum of the expected total accessibility of the PODs from the LDC and the expected total accessibility of the PODs from the demand locations.

**3.3.2. Equity.** We consider two types of equity in designing the last mile relief network: (i) *equitable accessibility* and (ii) *equitable supply allocation*.

We measure equitable accessibility in terms of *the minimum accessibility of the PODs* under each scenario, where the minimum is calculated over demand locations. In our model, we ensure equitable accessibility to the PODs from the demand locations by defining a coverage set for each demand location. The coverage set includes the candidate PODs that satisfy a minimum threshold requirement in terms of the accessibility scores associated with the links. In this way, each demand location is served by a POD that satisfies the minimum accessibility requirement.

SLMRND considers equitable supply allocation at the POD level. Equitable allocation of supplies among demand points is ignored at this point, since the relief personnel at the PODs usually make decisions regarding the final delivery amounts once the relief operations start. Therefore, in setting up the last mile relief network, it is sufficient to distribute supplies among PODs in a balanced way considering the capacity limitations. To measure and model equity in supply allocation, we compute the *maximum proportion of unsatisfied demand (MPUD)* under each scenario, where the maximum is calculated across the PODs.

### 3.4. Supply Allocation Policies

Different policies can be considered for allocating supplies equitably among the PODs when designing the last mile relief network. One of the common policies for dividing scarce supplies among recipients equitably is proportional allocation (e.g., Balcik et al. 2008;

(McCoy and Lee 2014). Similarly, we consider a strict proportional allocation policy (called the *PD Policy*) to determine the delivery amounts to PODs; that is, the available supply at the LDC is divided among the PODs in proportion to the total demand assigned to the PODs under each scenario. We also consider an alternative allocation policy (called the *TD Policy*), which relaxes the proportional allocation requirement but ensures that the shortage amount at each POD does not exceed a specified proportion of the corresponding total demand under each scenario; setting the proportion parameters equal for all PODs ensures equitable allocation (similar to Noyan 2010).

Both policies are used to control the shortage amounts at the POD level. Under each scenario, the PD policy enforces an equal proportion of unsatisfied demand (PUD) at each POD, whereas the TD policy introduces an upper bound on the MPUD. It can be analytically shown (see §4.2) that the model that incorporates the PD policy performs better than the one under the TD policy in terms of the equity metric MPUD. However, enforcing the proportional allocation can significantly compromise from the accessibility metric ETA. In this respect, we consider a relaxed PD policy, which aims at limiting the deviations from the strict PD policy. However, under the relaxed PD policy the proportions of unsatisfied demand at individual PODs can differ, and consequently, MPUD can be undesirably higher compared to the PD policy. To avoid such situations, we additionally impose the TD policy, which limits the MPUD value and performs better than the PD policy in terms of ETA. Thus, considering the strengths of the PD and TD policies, we design a *hybrid allocation policy* that can balance the trade-off between equity and accessibility. The resulting model, presented in §4.1, involves this hybrid allocation policy and can achieve high levels of accessibility and equity simultaneously. We also note that two special cases of the proposed model correspond to the models enforcing the PD policy and the TD policy.

## 4. SLMRND Modeling and Analysis

In this section, we present our modeling approach for SLMRND. In §4.1, we develop a stochastic programming model incorporating the hybrid allocation policy. In §4.2, we analyze the characteristics of the proposed model; in particular, we present two special cases and discuss the implications of the alternative supply allocation policies on accessibility and equity metrics.

### 4.1. Stochastic Optimization Model

We consider a network where each node represents a settlement in the affected region, and we denote the set of nodes by  $I$ . Additionally, we denote the

set of candidate PODs in the network by  $J$  and assume that  $J \subseteq I$ . The coverage sets are defined by enforcing a minimum threshold requirement on each accessibility score; we denote the common threshold value by  $\tau$ . We capture the inherent uncertainty in the network through a finite set of scenarios denoted by  $S$ . Each scenario represents the joint realization of the demands at the nodes and of the accessibility scores associated with the links of the network. Consequently, coverage sets are also scenario dependent. We provide a list of the scenario-dependent parameters below:

- $p^s$ : probability of scenario  $s \in S$ ;
- $d_i^s$ : demand at node  $i$  under scenario  $s$ ,  $i \in I$ ,  $s \in S$ ;
- $v_{0j}^s$ : score for accessibility to candidate POD  $j$  from the LDC under scenario  $s$ ,  $j \in J$ ,  $s \in S$ ;
- $v_{ij}^s$ : score for accessibility to candidate POD  $j$  from demand node  $i$  under scenario  $s$ ,  $i \in I$ ,  $j \in J$ ,  $s \in S$ ;
- $N_i^s = \{j \in J \mid v_{ij}^s \geq \tau\}$ : set of candidate PODs that can cover demand node  $i$  under scenario  $s$ ,  $i \in I$ ,  $s \in S$ ;
- $M_j^s = \{i \in I \mid v_{ij}^s \geq \tau\}$ : set of demand nodes that can be covered by the candidate POD  $j$  under scenario  $s$ ,  $j \in J$ ,  $s \in S$ .

As  $J \subseteq I$ , a sufficiently large number ( $V$ ) is assigned to  $v_{jj}^s$  so that the inequalities  $v_{jj}^s = V > \max_{i \in J} v_{ji}^s > \tau$  hold, which in turn implies that  $j \in N_j^s$  for all  $j \in J$ ,  $s \in S$ . In addition, we define the following deterministic parameters:  $\kappa$  denotes the maximum number of PODs to be opened ( $\kappa \leq |J|$ ),  $\Theta$  denotes the amount of total available supplies, and  $K_j$  represents the upper bound on the capacity of POD  $j$ . In practical settings, it is realistic to assume that the values of the parameters  $K_j$  are sufficiently large to allow a POD located at a demand node to serve at least its own location under any scenario. Therefore, in the rest of the paper, we make the assumption that

$$K_j \geq \max_{s \in S} d_j^s \quad \text{for all } j \in J. \quad (1)$$

As discussed before, last mile relief networks must be set up quickly before the uncertainties related to the post-disaster conditions are resolved. Therefore, a two-stage stochastic programming framework is suitable for the structure of SLMRND. In our two-stage modeling framework, the decisions on the locations and capacities of the PODs are made at the first stage before uncertainties in demands and accessibility scores are resolved. The decisions related to the allocation of supplies to the PODs, as well as the assignments of the demand points to the PODs are made at the second stage given the predetermined first-stage decision variables and the observed uncertain parameters. The following notation is used for the decision variables.

First-stage decision variables:

$y_j = 1$  if a POD is located at node  $j \in J$ , and  $y_j = 0$  otherwise;

$R_j$ : the capacity allocated to POD  $j \in J$  (i.e., an upper bound on the amount of supplies that can be delivered to POD  $j$ ).

Second-stage decision variables:

$x_{ij}^s = 1$  if demand node  $i \in I$  is served by POD  $j \in N_i^s$  under scenario  $s \in S$ , and  $x_{ij}^s = 0$  otherwise;

$r_j^s$ : the amount of supplies delivered to the POD  $j \in J$  under scenario  $s \in S$ .

As discussed in §3, SLMRND focuses on establishing accessible networks where the population groups are served equitably. In modeling SLMRND, we consider an approach that incorporates equitable supply allocation policies into the model through the constraints and focuses on an efficiency-related objective function featuring the total accessibility. Furthermore, equitable accessibility is ensured by assigning each demand point to a POD in its coverage set defined based on the minimum accessibility requirement. Thus, we enforce a lower bound (denoted by  $\tau$ ) on the minimum accessibility score over demand points (as an alternative to the “maximin” approach, which would maximize the minimum accessibility score). We note that the threshold parameter  $\tau$  can be used to balance the trade-off between the equity (in terms of the worst accessibility score) and efficiency (in terms of the total accessibility).

To impose the hybrid allocation policy, we first express the total demand assigned to POD  $j \in J$  under scenario  $s \in S$  (in terms of the assignment decisions) as follows:

$$\text{TD}_j^s \stackrel{\text{def}}{=} \sum_{i \in M_j^s} x_{ij}^s d_i^s.$$

Then, the corresponding proportional total demand is obtained by

$$\text{PD}_j^s \stackrel{\text{def}}{=} \frac{\theta^s}{\sum_{i \in I} d_i^s} \text{TD}_j^s, \quad (2)$$

where  $\theta^s$  denotes the total amount of delivery under scenario  $s$ ; it is calculated as  $\theta^s = \min(\Theta, \sum_{i \in I} d_i^s)$ .

We next present the two-stage stochastic programming model of SLMRND under the hybrid supply allocation policy (referred to as *Model\_Hybrid*). The formulation of the associated first-stage problem is given by

$$\text{maximize } \left\{ \sum_{j \in J} \bar{\nu}_{0j} y_j + E[Q(\mathbf{y}, \mathbf{R}, \xi)] \right\} \quad (3)$$

$$\text{subject to } \sum_{j \in J} y_j \leq \kappa, \quad (4)$$

$$R_j \leq K_j y_j, \quad j \in J, \quad (5)$$

$$y_j \in \{0, 1\}, \quad j \in J, \quad (6)$$

$$R_j \geq 0, \quad j \in J. \quad (7)$$

Here  $\bar{\nu}_{0j}$  denotes the expected accessibility from the LDC to POD  $j$ ; these expected values can be estimated by  $\sum_{s \in S} p^s \nu_{0j}^s$  for all  $j \in J$ . In addition,  $\xi$  denotes the random data and  $Q(\mathbf{y}, \mathbf{R}, \xi)$  is the objective function of the second-stage problem for a given set of first-stage decisions. For  $\xi^s = (\mathbf{d}^s, \mathbf{v}^s)$ , which represents the realization of the random data under scenario  $s \in S$ , the second-stage problem is formulated as follows:

$$Q(\mathbf{y}, \mathbf{R}, \xi^s) =$$

$$\text{maximize } \left\{ \sum_{i \in I} \sum_{j \in N_i^s} \nu_{ij}^s x_{ij}^s - \epsilon \sum_{j \in J} \beta_j^s \right\} \quad (8)$$

$$\text{subject to } r_j^s \leq R_j, \quad j \in J, \quad (9)$$

$$\sum_{j \in J} r_j^s = \theta^s, \quad (10)$$

$$\sum_{j \in N_i^s} x_{ij}^s = 1, \quad i \in I, \quad (11)$$

$$x_{ij}^s \leq y_j, \quad i \in I, j \in N_i^s, \quad (12)$$

$$x_{jj}^s \geq y_j, \quad j \in J, \quad (13)$$

$$x_{ij}^s \in \{0, 1\}, \quad i \in I, j \in N_i^s, \quad (14)$$

$$r_j^s \leq \text{PD}_j^s + \beta_j^s \leq \text{TD}_j^s, \quad j \in J, \quad (15)$$

$$\text{TD}_j^s - r_j^s \leq \rho \text{TD}_j^s, \quad j \in J, \quad (16)$$

$$r_j^s \geq 0, \quad \beta_j^s \geq 0, \quad j \in J. \quad (17)$$

The objective function (3) maximizes the ETA. We estimate the expected accessibility of the PODs from the demand locations by the sample averaging, i.e.,  $E[Q(\mathbf{y}, \mathbf{R}, \xi)] = \sum_{s \in S} p^s Q(\mathbf{y}, \mathbf{R}, \xi^s)$ . Constraint (4) ensures that the number of facilities is not larger than the specified limit, whereas constraint (5) imposes a maximum capacity limit for each POD to prevent oversized facilities. By constraint (9), the amount of supplies delivered to an open POD does not exceed the capacity of the POD. Constraint (10) ensures that the total amount of delivery is equal to the total available supplies, unless the total demand is less than this value. In addition, constraint (9) together with constraint (5) implies that there has to be a POD located at node  $j$  if there is any delivery to that node (i.e., if  $r_j^s > 0$  for at least one scenario). Constraints (11), (12), and (14) guarantee the connectivity of the network in such a way that each demand node is assigned to a single open POD. Moreover, constraint (13) ensures that a POD located at a demand node serves its own location; this constraint is generally satisfied automatically because of the large values of  $\nu_{jj}^s$  in the objective function (8). However, under extremely restrictive capacity limits, removing constraint (13) might result in serving some demand nodes from other PODs. The set of constraints (15)–(16) guarantees that the shortage amount at each POD is below a predetermined

proportion  $\rho$  of the total demand faced by the POD. Using a common proportion parameter  $\rho$  for all PODs ensures equitable allocation of supplies. Moreover, constraint (15) enforces a relaxed PD policy by allowing the variables  $\beta$  to take positive values. Penalizing such values of the variables  $\beta$  in (8) allows us to distribute supplies among PODs in proportion to their total demands as much as possible without enforcing the strict PD policy and compromising from ETA. For a sufficiently small value of the  $\epsilon$  parameter (e.g.,  $10^{-10}$ ), Model\_Hybrid attains the same level of ETA as the model under only the TD policy. By changing the value of the penalty parameter  $\epsilon \in [0, \infty]$ , the balance between the accessibility (in terms of ETA) and equity (in terms of MPUD) can be controlled. The rest of the constraints enforce nonnegativity and binary restrictions.

It is easy to see that if Model\_Hybrid is feasible then the following relation holds:

$$\rho \geq \rho^* \stackrel{\text{def}}{=} \max_{s \in S} \left( 1 - \theta^s / \sum_{i \in I} d_i^s \right). \quad (18)$$

Decision makers can use this relation to specify a reasonable value for  $\rho$  based on the values of available supplies and scenario demands. Moreover, if Model\_Hybrid is feasible then there exists an optimal solution with

$$R_j = \max_{s \in S} r_j^s, \quad \forall j \in J. \quad (19)$$

The relation (19) and the following result about the optimal number of selected PODs allow us to exploit the special structure of the proposed model and develop an effective solution algorithm.

**PROPOSITION 4.1.** *At any optimal solution of Model\_Hybrid we have  $\sum_{j \in J} y_j = \kappa$ .*

This proposition can easily be proved under the assumption given in (1). The rationale behind the proof can be briefly explained as follows. From any feasible solution with  $\sum_{j \in J} y_j < \kappa$  we can always construct another feasible solution, which satisfies  $\sum_{j \in J} y_j = \kappa$  and has a higher objective function value because  $\bar{v}_{0j} \geq 0$  and  $v_{jj}^s > \max_{i \in I} v_{ij}^s$  for all  $j \in J$ .

We can solve the proposed two-stage stochastic programming model using a decomposition-based algorithm (see §5) or directly using a standard mixed-integer programming solver. For the latter option, we formulate it as a large-scale mixed-integer linear program (MILP), which is referred to as the deterministic equivalent formulation (DEF) and presented in the online supplement (Appendix A) (available as supplemental material at <http://dx.doi.org/10.1287/trsc.2015.0621>).

**4.1.1. Practical Implementation.** To utilize the proposed model in practice, relief organizations must first generate demand and accessibility scenarios. The important factors to consider when developing these scenarios might depend on the particular disaster setting on hand. However, as we illustrate in our case study, it is possible to use widely available and low cost tools in collecting and processing the network and population related data. For example, coordinates of the affected locations, travel times, and relevant geographical characteristics can be obtained from online mapping services or geographic information systems. Moreover, if the affected area is part of a national population registration system, obtaining population and demographic data would be especially easy for local organizations (such as municipalities and civil societies) who are familiar with such databases. Therefore, it is highly recommended for an international relief agency to cooperate with local organizations for gathering population-related information. Based on these data and the initial assessments of the relief organizations about the post-disaster conditions and needs, one could construct a set of demand and accessibility scenarios that sufficiently capture the aftermath of the disaster. The second main piece of data to be fed into our model is the locations and maximum capacity limits of the candidate PODs. Depending on the situation, relief organizations should identify existing buildings and/or consider constructing tents/prefabricated structures that can serve as PODs. Again, getting recommendations from the local authorities while choosing the candidate PODs is of critical importance. Finally, the parameters regarding the maximum number of PODs and the expected amount of supplies to be distributed through the relief network must be set by the decision makers in relief organizations.

After gathering the data and setting the parameter values, the following approach can be applied to attain an implementable network design for post-disaster relief operations. First, given the set of scenarios, the two-stage model is run once to determine the (first-stage) decisions on the locations and capacities of the PODs, which can be directly implemented. Note that the set of scenarios that is used to develop the stochastic optimization models cannot be expected to include all possibilities that might occur in the future. Therefore, the relief organizations must proceed with only the first-stage decisions at this point. After getting more information on the post-disaster conditions (i.e., after the demand and network related uncertainties are resolved to some extent), the decision makers should construct a single scenario that reflects the post-disaster relief network conditions more accurately. Then, given this representative scenario and the first-stage decision variables determined previously, the second-stage problem is

solved once to obtain the decisions related to the allocation of supplies among the PODs and the assignments of the demand points to the PODs. In summary, this approach allows the relief organizations to make decisions exactly in two stages: the first stage provides a reasonable set of first-stage decisions by taking into account the potential possible future outcomes, and the second stage allows the decision makers to obtain better recourse decisions by considering a more representative scenario.

#### 4.2. Model Analysis

In this section, we provide some observations and results to highlight the significance of the proposed model under the hybrid allocation policy. In particular, we investigate the implications of the alternative supply allocation policies on the performance metrics of interest. We commence by presenting the two relevant special cases (the models under the PD policy and the TD policy) of the Model\_Hybrid.

*Special case under the PD policy (referred to as Model\_PD).* We set  $\beta_j^s = 0$  for all  $j \in J$  and  $s \in S$ , and consequently, constraint (15) becomes

$$r_j^s \leq \text{PD}_j^s, \quad j \in J. \quad (20)$$

In this case, we can easily prove that constraint (20) holds with equality at any feasible solution of Model\_Hybrid, which ensures the strict proportional distribution (due to the constraint (10)). It is important to note that setting  $\beta_j^s = 0$  for all  $j \in J$  and  $s \in S$  is not equivalent to setting  $\epsilon$  to a very large constant (ideally,  $\infty$ ); in the latter approach the  $\beta_j^s$  variables can still take positive values (when there is no feasible solution satisfying (20) with equality because of the restrictive capacity limits).

*Special case under the TD policy (referred to as Model\_TD).* We set  $\epsilon = 0$ , or trivially, drop the decision variables  $\text{PD}_j^s$  and  $\beta_j^s$  from Model\_Hybrid; consequently, constraint (15) becomes

$$r_j^s \leq \text{TD}_j^s, \quad j \in J.$$

The hybrid model and its two special cases would provide the same solutions in rare cases when the relief supplies in the last mile network are ample compared to the total demand (i.e.,  $\text{TD}_j^s = \text{PD}_j^s$ ,  $j \in J$ ,  $s \in S$ ). Additionally, we observe that the values of the parameters  $K_j$  have significant importance in the performance of these alternative allocation policies. We first consider the trivial case where the parameters  $K_j$  are sufficiently large to make the related POD capacity constraints redundant.

**OBSERVATION 4.1.** Suppose that the parameters  $K_j$  are sufficiently large to make the related capacity constraints redundant, that is, assume that  $r_j^s \leq K_j$ ,  $j \in J$ ,  $s \in S$  holds for any second-stage feasible solution. Then, all three policies lead to the same optimal objective value, and moreover, Model\_Hybrid and Model\_PD are equivalent.

The rationale behind Observation 4.1 can be explained as follows. Suppose that we solve Model\_TD and obtain an optimal policy. Given the optimal assignment variables  $x$ , we can easily modify the variables  $r$  and  $R$  (based on (2) and (19), respectively) to construct an alternate optimal solution at which the proportional distribution is ensured. Observe that the first-stage objective function does not involve the modified variables  $r$  and  $R$ , and the optimal  $y$ - and  $x$ -decisions do not need to be altered because there are no upper bounds on the POD capacities. Therefore, we can always construct an alternate optimal solution of Model\_TD with  $r_j^s = \text{PD}_j^s$ ,  $j \in J$ ,  $s \in S$ , which is also an optimal solution of Model\_PD.

According to Observation 4.1, the hybrid policy does not provide an additional benefit under the trivial case. We next discuss the significance of the hybrid model for the nontrivial (and more realistic) case where the parameters  $K_j$  can have an effect on the optimal last mile relief network design decisions. To this end, we first provide the following interesting result related to the performance of the alternative allocation policies in terms of the equity metric of interest.

**PROPOSITION 4.2.** The random MPUD associated with a feasible solution of Model\_PD is stochastically dominated by the random MPUD associated with any feasible solution of Model\_TD in the first order.<sup>2</sup> In other words, the random MPUD associated with a feasible solution of Model\_PD is stochastically smaller.

**PROOF.** Consider a feasible solution of Model\_PD and let  $\hat{J}$  denote the set of selected PODs, i.e.,  $\hat{J} = \{j \in J : y_j = 1\}$ . We focus on the PUD at each selected POD, since the PUD associated with the unselected PODs is trivially 0 with certainty. Based on (2), for any feasible solution of Model\_PD we can calculate the corresponding PUD at POD  $j \in \hat{J}$  under scenario  $s$  (denoted by  $\hat{\rho}_j^s$ ) as follows:

$$\hat{\rho}_j^s = \frac{\sum_{i \in M_j^s} x_{ij}^s d_i^s - r_j^s}{\sum_{i \in M_j^s} x_{ij}^s d_i^s} = \frac{\sum_{i \in M_j^s} x_{ij}^s d_i^s - \text{PD}_j^s}{\sum_{i \in M_j^s} x_{ij}^s d_i^s} = 1 - \frac{\theta^s}{\sum_{i \in I} d_i^s}, \\ j \in \hat{J}, s \in S. \quad (21)$$

Note that we have  $\sum_{i \in M_j^s} x_{ij}^s d_i^s > 0$  for any POD  $j \in \hat{J}$  because  $x_{jj}^s = 1$  when  $y_j = 1$ . Then, it follows that at any feasible solution of Model\_PD we have

$$\max_{j \in \hat{J}} \hat{\rho}_j^s = 1 - \theta^s / \sum_{i \in I} d_i^s, \quad s \in S. \quad (22)$$

<sup>2</sup> A random variable  $X$  dominates another random variable  $Y$  in the first order if  $P(X \leq \eta) \leq P(Y \leq \eta)$  for all  $\eta \in \mathbb{R}$ . For details on the concept of first-order stochastic dominance we refer the reader to Müller and Stoyan (2002).

Now suppose that there is a feasible solution of Model\_TD with  $\max_{j \in \hat{J}} \hat{\rho}_j^s < 1 - \theta^s / \sum_{i \in I} d_i^s$  under a scenario  $s$ . According to (21), this can be the case only if  $r_j^s > PD_j^s$  holds for all  $j \in \hat{J}$ . Then, we would have  $\sum_{j \in \hat{J}} r_j^s > \sum_{j \in \hat{J}} PD_j^s$ , implying  $\sum_{j \in \hat{J}} r_j^s > \sum_{j \in \hat{J}} PD_j^s = \theta^s$ , i.e., the constraint (10) is violated. This contradicts the feasibility of the solution under consideration, and proves that for any feasible solution of Model\_TD the corresponding MPUD under  $s \in S$  is greater than or equal to  $1 - \theta^s / \sum_{i \in I} d_i^s$ . Then, the assertion follows trivially from the fact that the smallest value of MPUD under each scenario is attained at any feasible solution of Model\_PD (see (21) and (22)).  $\square$

Proposition 4.2 shows that the PD policy leads to the best performance in terms of MPUD. In fact, the PUD associated with a feasible solution of Model\_PD is the same for all of the open PODs under each scenario, and the constraint (16) becomes redundant for any reasonable value of  $\rho$  (i.e.,  $\rho \geq \rho^*$ ). Moreover, even setting  $\rho = \rho^*$  in Model\_TD would not be sufficient to guarantee the proportional distribution of supplies, since forcing the maximum proportion value to be less than or equal to  $\rho^*$  is not sufficient to ensure an equal PUD value at each POD. However, imposing such a restrictive proportional distribution policy might lead to a significant reduction in ETA. This trade-off becomes even more important when the capacity restrictions of PODs are more severe. In this respect, one can impose the relaxed version of the PD policy, which aims at minimizing the deviations from the strict PD policy (by minimizing the values of the nonnegative variables  $\beta_j^s$ ). However, in this relaxation-based approach, the PUD values at individual PODs can differ, and consequently, MPUD can be undesirably higher compared to Model\_PD (as also shown in Figures 5(b) and 6(b) in §6.2 for larger values of  $\rho$ ). Therefore, enforcing the TD policy in addition to the relaxed PD policy is essential for improving equity in terms of MPUD. As a result, the proposed model involving the hybrid policy can achieve high levels of accessibility and equity simultaneously.

## 5. The Integer L-Shaped Method

We develop a decomposition-based branch-and-cut algorithm to solve our two-stage stochastic mixed-integer programming model. As discussed in §2, several generic decomposition-based algorithms have been developed to solve such models. However, if possible, adapting a solution method that exploits the special structure of the problem would be preferable to develop a computationally effective algorithm. Along these lines, we utilize the integer L-shaped method, which is specifically suitable for stochastic programming programs with pure binary decision

variables in the first stage and mixed-integer variables in the second stage; furthermore, the method allows all of the second-stage parameters to be random. Even though our proposed model originally involves mixed-binary decision variables in the first stage, we can reformulate it so that the integer L-shaped method is applicable. We implement an enhanced version of the classical integer L-shaped method by employing state-of-the-art computational features, such as the lazy constraint callback of CPLEX and a parallelization of the Benders subproblems via the Boost C++ Libraries. To the best of our knowledge, devising such an enhanced integer L-shaped method is a first in the literature. Moreover, we use scenario-dependent cuts (multi-cuts) instead of aggregated cuts (single-cuts) in approximating the expected second-stage objective function value. Below, we explain our Benders decomposition-based branch-and-cut algorithm in detail.

According to (19), we can retrieve the optimal values of the variables  $R_j$  from the given optimal second-stage variables. In this spirit, we can delete the variables  $R_j$  from the first-stage problem and replace  $R_j$  by  $K_j y_j$  in the second-stage problem to guarantee the satisfaction of the capacity constraints (5) and (9). Following this approach, with some abuse of notation, we denote the objective function of the second-stage problem under scenario  $s$  by  $Q(\mathbf{y}, \xi^s)$  instead of  $Q(\mathbf{y}, \mathbf{R}, \xi^s)$  when describing the algorithm. In other words, we drop the variables  $R_j$  and focus on the equivalent formulation of the proposed model, which involves only the pure binary variables  $y_j$  in the first stage.

Here we describe our solution algorithm considering a general representation of the second-stage problem:

$$Q(\mathbf{y}, \xi^s) = \underset{\mathbf{z}}{\text{maximize}} \left\{ (\mathbf{q}^s)^T \mathbf{z}: W^s \mathbf{z} = \mathbf{h}^s - T^s \mathbf{y}, \right. \\ \left. \mathbf{z} \in \mathbb{R}^{n_1} \times \{0, 1\}^{n_2} \right\}. \quad (23)$$

At a given iteration of the multi-cut integer L-shaped algorithm, the following *relaxed master problem* (RMP) is considered:

$$(RMP) \quad \underset{\mathbf{y}}{\text{maximize}} \left\{ \sum_{j \in J} \bar{\nu}_{0j} y_j + \sum_{s \in S} p^s \vartheta^s \right\} \quad (24)$$

$$\text{subject to } \sum_{j \in J} y_j = \kappa, \quad (25)$$

$$\mathbf{D}_l \mathbf{y} \leq d_l, \quad l = 1, \dots, t_1, \quad (26)$$

$$\mathbf{E}_l^s \mathbf{y} + \vartheta^s \leq e_l^s, \\ l = 1, \dots, t_2, s \in S, \quad (27)$$

$$\mathbf{y} \in [0, 1]^{|\mathcal{J}|}, \quad \vartheta \in \mathbb{R}^{|S|}. \quad (28)$$

We obtain this RMP from three types of relaxations of the two-stage model: the integrality restrictions on

the variables  $y_j$  are relaxed, the feasibility requirements of the second-stage problems are relaxed, and the exact calculation of the second-stage objective values is relaxed. In the formulation of the RMP,  $t_1$  and  $t_2$  designate the number of feasibility and optimality cuts generated so far, respectively. The so-called *feasibility cuts* (26) are used to represent the conditions for the feasibility of the second-stage problems. The auxiliary variables  $\vartheta^s$ ,  $s \in S$ , together with the *optimality cuts* (27), denote appropriate approximations of  $Q(\mathbf{y}, \xi^s)$ ,  $s \in S$ . Note that relaxing the integrality restrictions on the variables forms the basis of a branch-and-cut algorithm, whereas relaxing the exact calculation of  $Q(\mathbf{y}, \xi^s)$ ,  $s \in S$ , via a polyhedral representation is the key step of the *L-shaped method*. We next derive the particular forms of the Benders (feasibility and optimality) cuts that are valid for our model.

**PROPOSITION 5.1.** *Let  $y_j = 1$ ,  $j \in H_l$ , and  $y_j = 0$ ,  $j \notin H_l$  be the  $l$ th first-stage feasible solution that leads to an infeasible second-stage problem. Then, the following feasibility cut is valid:*

$$\sum_{j \in H_l} y_j \leq \kappa - 1. \quad (29)$$

**PROOF.** As  $\sum_{j \in J} y_j = \kappa$  at any first-stage feasible solution (Proposition 4.1), we have  $|H_l| = \kappa$ . This clearly shows that  $\sum_{j \in H_l} y_j \leq \kappa$  for any binary vector  $\mathbf{y}$ , and the equality holds only for the  $l$ th feasible solution. Thus, (29) is violated only by the  $l$ th feasible solution.  $\square$

For any given first-stage solution we can calculate the second-stage objective values, and by the boundedness of the second-stage model there exist finite values  $U^s$ ,  $s \in S$ , such that

$$U^s \geq \underset{\mathbf{y}}{\text{maximize}} \left\{ Q(\mathbf{y}, \xi^s) : \sum_{j \in J} y_j = \kappa, \mathbf{y} \in \{0, 1\}^{|J|} \right\}, \quad s \in S. \quad (30)$$

In this setting, the optimality cuts (single-cuts) proposed in Laporte and Louveaux (1993) are valid for our model, but fortunately, we derive stronger and multi-cut versions of those optimality cuts by exploiting the special structure of the proposed mathematical programming formulation.

**PROPOSITION 5.2.** *Let  $y_j = 1$ ,  $j \in H_l$ ,  $y_j = 0$ ,  $j \notin H_l$ , be the  $l$ th first-stage feasible solution, and  $\varrho_l^s$  the corresponding optimal objective function value of the second-stage problem for scenario  $s \in S$ . Then, the following set of optimality cuts is valid:*

$$\vartheta^s \leq (U^s - \varrho_l^s) \left( \kappa - \sum_{j \in H_l} y_j \right) + \varrho_l^s, \quad s \in S. \quad (31)$$

**PROOF.** As mentioned in the proof of Proposition 4.1,  $\kappa - \sum_{j \in H_l} y_j \geq 0$  for any first-stage feasible

binary vector  $\mathbf{y}$ , and it takes the value 0 only for the  $l$ th feasible solution. In the latter case, the right-hand side reduces to  $\varrho_l^s$ , and as desired, (31) cuts the  $l$ th first-stage feasible solution if  $\vartheta^s > \varrho_l^s$  for at least one scenario  $s \in S$ . For any other first-stage feasible solution, we have  $|H_l| < \kappa$  and the term  $(\kappa - \sum_{j \in H_l} y_j)$  takes a positive integer value, say  $\varepsilon$  (i.e.,  $\varepsilon \geq 1$ ). Then, the right-hand side becomes  $\varepsilon U^s - (\varepsilon - 1)\varrho_l^s \geq U^s$  for all  $s \in S$  because  $U^s \geq \varrho_l^s$  by the definition of  $U^s$ . Thus, in this case the optimality cuts (31) are redundant.  $\square$

It is easy to show that any feasibility cut that is valid for the two-stage model with the *continuous relaxation* of the second-stage problem is also valid for the original model involving integers in the second stage. Furthermore, any continuous *L-shaped* optimality cut associated with scenario  $s$  provides an upper bound on  $Q(\mathbf{y}, \xi^s)$ . These two observations (Laporte and Louveaux 1993) allow us to use both feasibility and optimality cuts, which are originally derived for the continuous *L-shaped* method, to obtain stronger formulations of the RMP. Utilizing the representation in (23), the continuous feasibility cuts are given by

$$(\mathbf{v}^{ls})^T (\mathbf{h}^s - T^s \mathbf{y}) \geq 0, \quad (32)$$

and the continuous optimality cuts are in the form of

$$\vartheta^s \leq (\boldsymbol{\pi}^{ls})^T (\mathbf{h}^s - T^s \mathbf{y}), \quad s \in S. \quad (33)$$

Here  $\boldsymbol{\pi}^{ls}$  denotes an optimal solution of the dual problem of the continuous relaxation of the second-stage problem under scenario  $s$  given the  $l$ th first-stage feasible solution, whereas  $\mathbf{v}^{ls}$  denotes an extreme ray of the corresponding dual feasible region. For a detailed discussion on the continuous *L-shaped* method, we refer the reader to Birge and Louveaux (1997). Keep in mind that these cuts themselves are not sufficient to guarantee the convergence to an optimal solution, therefore they must be accompanied by both (29) and (31). However, we observed that incorporating these cuts significantly improves the performance of the algorithm.

Note that we can easily aggregate the optimality cuts of the form (31) (similarly, (33)), which we refer to as multi-cuts, and obtain their single-cut versions. In particular, we obtain single-cuts by using the weighted sum of multi-cuts where the weights are the corresponding probabilities. The multi-cut approach avoids the loss of the information associated with each realization of the second-stage problem, and it is generally expected to improve the approximations and reduce the number of iterations with respect to the single-cut method. However, in the classical implementation of the Benders decomposition with multi-cuts, the size of the relaxed master problem may

cause computational difficulties, since we add a large number of optimality cuts at once. Fortunately, this drawback is addressed by the lazy constraint callback feature in our enhanced implementation, and we drop the single-cut versions completely out of consideration in our study.

### 5.1. Computing Upper Bounds on the Second-Stage Objective Values

The upper bounds  $U^s$ ,  $s \in S$ , featured in the optimality cuts (31) have a significant impact on the computational performance of the algorithm. The smaller valid upper bound values obviously lead to stronger formulations of the RMP, and consequently, a fast discovery of an optimal solution. We initialize the algorithm by computing an appropriate upper bound on the optimal second-stage objective value for each scenario. To this end, we opt for solving the following problem under each scenario  $s \in S$ :

$$\underset{\mathbf{y}, \mathbf{x}^s}{\text{maximize}} \left\{ \sum_{i \in I} \sum_{j \in N_i^s} \nu_{ij}^s x_{ij}^s : \sum_{j \in J} y_j = \kappa, \mathbf{y} \in \{0, 1\}^{|J|}, (11) - (14) \right\}. \quad (\text{InitP}_s)$$

It is easy to see that  $\text{InitP}_s$  provides a valid upper bound, i.e., its optimal objective function value is bigger than or equal to the right-hand side of (30) because we consider a relaxed version of the second-stage problem by ignoring the constraints related to the equitable supply allocation. Furthermore, to enhance computational performance, we update these bounds during the course of the algorithm according to the upper bounding scheme presented in Laporte and Louveaux (1993). Specifically, we determine the new bounds for any finite value  $t \geq 1$  as follows:

$$U^s = \max_{\vartheta^s, \mathbf{y}} \left\{ \vartheta^s : \sum_{j \in J} y_j = \kappa, \mathbf{y} \in \{0, 1\}^{|J|}, \text{ and } (\vartheta^s, \mathbf{y}) \text{ satisfies (33) for } l=1, \dots, t \right\}. \quad (34)$$

We update the current upper bounds if they are larger than the corresponding values in (34).

### 5.2. Implementation of the Algorithm Using the Lazy Constraint Callback

In the classical Benders decomposition approach, the RMP is solved to optimality and then the feasibility and optimality cuts associated with the current optimal solution are added to the RMP before it is reoptimized. This iterative process is repeated until the optimality gap is smaller than a prespecified tolerance level. Following this mainstream implementation of the Benders decomposition, the original integer *L*-shaped method first aims to maintain the feasibility of the second-stage problems, then creates branches based on a fractional variable in the optimal solution of the RMP. Finally, at a candidate incumbent (best

available feasible) solution it focuses on the correctness of the approximation of the expected second-stage objective value. The primary drawback of this classical implementation is that a new search tree must be constructed every time the RMP is solved, and such a scheme may result in reevaluating the same nodes over and over again. Alternatively, we have followed a recent approach, described by Rubin (2011), that allows us to execute the entire algorithm on a *single search tree* by utilizing the *lazy constraint callback* feature of CPLEX (IBM ILOG CPLEX 2013). In contrast to the classical integer *L*-shaped algorithm, whenever a candidate incumbent solution is identified in the search tree, the associated missing Benders cuts are appended to the RMP as *lazy constraints*. With this labeling, the solver is informed that most generated constraints are not expected to be active at the optimal solution. In fact, the solver enforces the generated Benders cuts as it deems necessary. Therefore, the number of cuts appended during the course of the algorithm will not cause significant deterioration in the computational performance of the algorithm. The only major drawback of this approach is the incompatibility of the control callbacks (in our case the lazy constraint callback) and the *dynamic search* feature of CPLEX.

In our implementation, the lazy constraint callback routine is invoked whenever the branch-and-cut algorithm finds a candidate incumbent solution in the search tree. The callback routine either identifies a missing feasibility or optimality cut violated by the candidate incumbent solution and introduces it as a lazy constraint or certifies the candidate solution as the new incumbent. This scheme, in fact, ensures that no integer solution is evaluated multiple times during the course of the algorithm. Recall that the RMP involves only the first-stage decision variables, and it does not guarantee the feasibility of the second-stage problems. To ensure the existence of feasible second-stage solutions, we need to identify a missing feasibility cut for each candidate incumbent solution. To save computational effort in checking the feasibility of the second-stage problems, we carry out a three-phase procedure described in Algorithm 1. If, given the candidate solution, second-stage infeasibility for a scenario is encountered at one of the phases, we generate the corresponding feasibility cuts of types (29) and (32).<sup>3</sup> Note that it is sufficient to generate the feasibility cut (32) for the first infeasible scenario encountered. Moreover, solving the continuous relaxations in phase 2 is not an additional computational burden,

<sup>3</sup>Instead of using the feasibility cuts, one can opt to use the *reject()* method in the *incumbent callback* function to remove the undesired solutions from consideration.

because it would eventually be necessary for generating the continuous optimality cuts when all of the second-stage problems are feasible. When the infeasibility is detected in phase 1 or CPLEX encounters an infeasible problem using its probing algorithms in phase 2, we solve the infeasible second-stage problem with the *presolve* feature disabled to obtain a corresponding extreme ray featured in (32). In case all of the second-stage problems turn out to be feasible, we check whether there is any missing optimality cut, and if necessary generate the corresponding optimality cuts to correctly approximate the expected second-stage objective value associated with the candidate first-stage solution. To this end, we solve all of the second-stage problems to optimality, and for any second-stage problem with an optimal objective value smaller than the current optimal value of  $\hat{\vartheta}^s$  we append the optimality cuts (31) and (33). At every candidate solution that leads to second-stage feasibility, we also solve the problem (34) to obtain the new upper bounds  $U^s$ ,  $s \in S$ . Once all of the appended lazy constraints are satisfied in the RMP, the candidate solution is considered as incumbent. The branch-and-cut algorithm continues until the incumbent is proved to be optimal. The pseudocode of our finite exact algorithm is presented in Algorithm 2.

#### Algorithm 1 (Procedure *check\_feasibility*)

```

1 for  $s \in S$  do
2   // Phase 1. Probing routine
3   Given the  $y$ -variables check whether
4     constraints (11) and (12) are conflicting; in
5     particular, identify if there are demand
6     nodes that cannot be covered by any open
7     POD;
8   if all the demand nodes can be covered by an
9     open POD then
10    // Phase 2. Check the feasibility of
11      the continuous relaxation problem
12    Solve the continuous relaxation of the
13      second-stage problem under scenario  $s$ ;
14    if continuous relaxation is feasible then
15      Retrieve  $\pi^{sl}$ ;
16      // Phase 3. Feasibility problem
17      Solve the feasibility problem under
18        scenario  $s$  (we simply replace the
19          objective function (8) by a constant
20          to check whether a feasible
21          solution can be obtained);
22      if not feasible then Infeasibility
23        detected, break;
24      else Infeasibility detected, break;
25    else Infeasibility detected, break;
26  end
```

REMARK 5.1. In our implementation, we add an optimality cut in line (10) of Algorithm 2 if  $\hat{\vartheta}^s -$

$\hat{\vartheta}^s > 10^{-6}$  and  $(\hat{\vartheta}^s - \hat{\vartheta}^s)/\hat{\vartheta}^s > 10^{-4}$ . Moreover, we note that the upper bound values in the constraints generated in line (2) cannot be updated automatically. Therefore, during the course of the algorithm, we generate additional cuts of the same form with the updated upper bounds whenever there is a reasonable improvement (e.g., %0.02) in the average upper bound value ( $\sum_{s \in S} p_s U_s$ ).

#### 5.3. Parallel Computing

Throughout our implementation, we employ parallel computing techniques to enhance the computational performance of the algorithm. To this end, we benefit from two parallelization strategies. The first strategy is to distribute independent operations (such as solving the second-stage problems and the initialization problems) among the available threads to exploit the advantages of our decomposition approach. The second strategy is to use the built-in parallel programming features of CPLEX to solve a single problem. In particular, these techniques involve the evaluation of the nodes in the branch-and-cut tree of a mixed-integer program in parallel, or the optimization of linear programs using concurrent optimizers (IBM ILOG CPLEX 2013). To implement the first and second strategy, we use the Boost C++ Libraries and adjust the *threads* parameter of CPLEX, respectively.

In our implementation, we set the number of threads in a way that at most eight threads can be used at the same time. To accelerate the discovery of feasible solutions in the branch-and-cut tree of the RMP, we allocate two threads to CPLEX (line 5 of Algorithm 2). Additionally, we switch the *parallel mode* option of CPLEX to *opportunistic*, which reduces the synchronization times of the threads at the expense of nondeterministic solution times. In contrast to the RMP, the initialization problems and the second-stage problems are not computationally demanding; therefore, we disable the parallelization features of CPLEX while solving these problems. Instead, we follow the first strategy and distribute these problems among the multiple threads to reduce the computational burden of solving  $|S|$  problems. Note that we can solve up to eight initialization problems concurrently (line 1 of Algorithm 2) as the branch-and-cut has not been initiated yet. However, once the branch-and-cut begins, the number of second-stage problems that can be solved concurrently (line 9 of Algorithm 2) is limited to four. We also allow CPLEX to use four threads while solving the problem (34) (line 8 of Algorithm 2).

## 6. Computational Study

To test our model and algorithm, we construct a case study based on real-world data from the 2011 Van earthquake. In §6.1, we explain the data generation

**Algorithm 2** (Enhanced integer L-shaped algorithm)

```

// Initialization
1 Set  $t_1 = t_2 = 0$ . Solve  $\text{InitP}_s$  for all  $s \in S$  to obtain the upper bounds  $U^s, s \in S$ ;
2 Enforce the upper bounds on the variables  $\vartheta^s$  by adding the following constraints to the RMP:
    $\vartheta^s \leq U^s, \forall s \in S$ ;
// Main loop
3 Invoke CPLEX to solve the RMP and initiate branch-and-cut procedure;
4 while CPLEX determines that both the relative and absolute optimality gaps of the current incumbent are greater
   than the specified thresholds do
5   Identify a new candidate incumbent solution  $(\hat{y}, \hat{\vartheta})$ ;
6   all_feasible = check_feasibility( $\hat{y}$ ); if all_feasible then
7     for  $s \in S$  do
8       Solve the problem (34) to calculate the new upper bound, and update the current bound
         if possible;
9       Solve the second-stage problem under scenario  $s$  to optimality and let  $\hat{\varrho}^s, s \in S$ , denote the
         optimal second-stage objective values;
10      if  $\vartheta^s > \hat{\varrho}^s$  then //  $\hat{y}$  violates some of the missing optimality cuts
11        Add the corresponding optimality cuts of the form (31) and (33) to the RMP as lazy
           constraints;
12      end
13    end
14  else //  $\hat{y}$  violates some of the missing feasibility cuts
15    Solve the continuous relaxation of the first infeasible second-stage problem without presolve,
      retrieve  $\mathbf{v}^{ls}$  utilized in (32);
16    Add the corresponding feasibility cuts of the form (29) and (32) to the RMP as lazy constraints;
17  end
18 end

```

process, and in §6.2 we present computational results to illustrate the significance of the proposed model. In §6.3, we provide results for evaluating the performance of the solution algorithm.

### 6.1. Data Set Generation

A severe earthquake hit eastern Turkey near the urban center of Van province on October 23, 2011. Thousands of residential units collapsed or were severely damaged, some of which collapsed after the aftershock on November 9, 2011. More than 600 people died, 2,500 were injured, and about 600,000 people were affected by these two earthquakes (IFRC 2012). The response of relief organizations and the donor community was prompt to meet the urgent needs of the affected people; nevertheless, mostly because of coordination-related problems, some people did not have access to sufficient aid. The Van earthquake relief case indicates the importance of establishing a systematic aid delivery system for ensuring a successful disaster response. Below, we summarize the steps followed to collect and process the real-world data obtained for the affected region.

**I. Data Collection: Network and Population.** The network contains a single LDC and the 94 settlements affected by the earthquake in the main district

of Van. The coordinates of the nodes and the travel times are obtained from a free online mapping service (Google Maps). The population and demographic data for each settlement (such as the elderly, children, disabled, and female proportions) are obtained from the national address-based population registration system (Turkish Statistical Institute (TUIK) 2012).

**II. Clustering the Settlements.** To test the performance of the proposed algorithm on a variety of instances, we create new networks with 30 and 60 nodes by clustering the demand nodes of the original 94-node network. For clustering, we use a  $p$ -median model, which minimizes the total demand-weighted travel times. The population and demographic data related to each cluster are aggregated and assigned to the cluster centroid. As an example, the clusters and cluster centroids for the 30-node network are depicted in Figure 2. Although our solution algorithm can solve the 94-node instances with 50, 100, and 200 scenarios in reasonable times (see §6.3), we use the solutions of the smaller network with 30 nodes and 50 scenarios in §6.2 for illustrative purposes. In general, clustering would also be useful when the networks in consideration are too large to be solved efficiently. If the demand nodes are reasonably close to each other (e.g., in dense/urban networks), the information loss

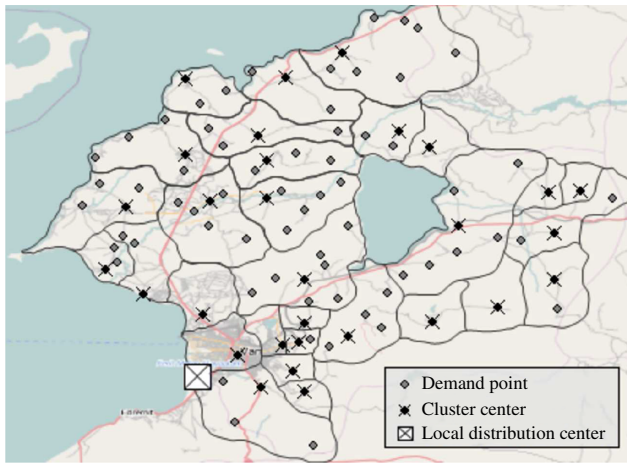


**Figure 2** (Color online) Example of Clustered Network (30 Clusters)

Source. OpenStreetMap, 2013. © OpenStreetMap contributors, <http://www.openstreetmap.org/#map=10/38.5841/43.3397>, accessed August 31, 2013.

due to clustering would be small. For instance, the affected region after the Van earthquake is moderately dense, and the maximum travel time from an original demand node to the centroid of the corresponding cluster is 29 minutes for the 30-node network. Otherwise (e.g., in dispersed/rural networks), the cluster centroids may not represent all demand nodes with sufficient accuracy; in that case the decision makers may consider locating multiple centroids in large clusters or use a  $p$ -center model to better control the clustering bias.

**III. Estimating the Base Demand.** We estimate the number of affected people in each cluster based on the damage intensity levels of the clusters. The damage intensity levels are estimated using a formula that expresses the intensity in terms of the distance to the fault line and the surface wave magnitude of the earthquake (Erdik and Eren 1983); see the online supplement (Appendix B.1) for the formula. In our case study, we consider three damage intensity levels ("destructive," "damaging," and "very strong or strong") around the epicenter of the earthquake (see Figure 1 in Appendix B.1 of the online supplement). Based on these damage intensity levels, we estimate the percentage of total households affected by the earthquake at three possible damage states: "No damage (ND)"; "Slight and medium damage (MD)"; "Heavy damage and collapse (HD)" (see Appendix B.1 of the online supplement for the estimated percentages). We assume that the proportion of the affected population in each cluster is equal to the percentage of affected households, and estimate the base demand for supplies as a weighted combination of the affected populations at different damage states. The weights associated with the damage states ND, MD, and HD are specified as 0, 0.5, and 1, respectively.

**IV. Estimating the Base Accessibility Scores.** The following steps are applied to calculate the base values of the accessibility scores in each test network.

1. We obtain the *travel times* between each pair of nodes from Google Maps, which considers the physical characteristics (such as the type and grade level) of the roads (Barth 2009).

2. Some areas of the affected region are close to Lake Van, which poses flooding risks on some roads. We estimate a *risk score* for each link based on its distance from the lake (see Appendix B.2 in the online supplement for details). Accordingly, these risk scores are higher for the links in more risky areas.

3. To incorporate the demographic characteristics in the calculation of the scores for the accessibility to PODs from the demand locations, we assign a *mobility score* to each demand node (higher scores correspond to lower mobility). The mobility score of a demand node is calculated as the weighted sum of the proportions (with respect to the total population in the entire area) of disabled people, elderly, and women with children at that node, where the weights are specified as 0.5, 0.3, and 0.2, respectively.

4. We use the reciprocal of the product of the travel time, risk score, and mobility score to calculate the scores for the accessibility to PODs from the demand locations. On the other hand, we ignore the mobility score for the accessibility to PODs from the LDC. If preferred, one can use a different type of decreasing function to obtain the accessibility scores.

**V. Generating Demand and Accessibility Scenarios.** Given the base values for demands and accessibility scores, we generate the realizations of the random demand and accessibility parameters to construct a set of scenarios that represent the post-disaster relief network conditions. In generating these realizations, it is crucial to consider the dependency structure in the relief network; the demand and the damage in the network infrastructure would be higher for regions closer to the epicenter of the earthquake. To account for this, as in III, we consider three damage intensity levels. Then, we obtain the realizations under each scenario by multiplying the base values of the demands and accessibility scores by randomly generated deviation factors; this random generation scheme depends on the damage intensity levels (see Appendix B.3 in the online supplement for details).

**VI. Other Input Parameters.** We explain how we set the values of the input parameters  $\tau$ ,  $\kappa$ ,  $\Theta$ ,  $K_j$ , and  $\rho$ . We specify the value of  $\tau$  based on the number of demand nodes that are difficult to be covered (i.e., the demand nodes with small  $|N_i^s|$ ). More specifically,  $\tau$  is set by limiting the number of demand points whose coverage set includes less than a certain number of candidate PODs. For this, we consider

the worst (smallest) possible values of the realizations of the accessibility scores (denoted by  $\hat{v}_{ij}$ ) and set the value of  $\tau$  based on the following condition:

$$|\{i \in I : |N_i| = |\{j \in J \mid \hat{v}_{ij} \geq \tau\}| \leq \lceil \gamma_1 |J| \rceil\}| < \lceil \gamma_2 |I| \rceil.$$

For our 30-node case study network, we set  $\gamma_1 = 0.05$  and  $\gamma_2 = 0.15$ , and observe that the above condition is satisfied for  $\tau \in [0, 0.04]$ . From these possible values, we select 0.01, 0.02, and 0.03 as low, medium, and high accessibility thresholds. We note that  $\tau < 0.01$  is too small to enforce an acceptable level of accessibility, whereas  $\tau > 0.03$  in general leads to infeasibility due to the capacity limitations.

In practice, the parameter  $\kappa$  can be set by the decision makers based on the available resources (i.e., budget, personnel, etc.). The parameter  $\kappa$  is selected as 6, 9, and 12, for the networks with 30, 60, and 94 nodes, respectively. The amount of available supplies  $\Theta$  is set at 90% of the expected total demand, which is calculated by multiplying the base values of the demand by the expectations of the specified uniform distributions (e.g., by  $(0.75 + 1.3)/2$  for the nodes in areas with “destructive” intensity level). To investigate the impact of the capacity upper bounds, we consider different levels as  $K_j = c\hat{d}_j$  in our analysis, where  $c$  takes values in the range [1.3, 4.75] and  $\hat{d}_j$  denotes the estimated base value of the demand at node  $j$ . We note that the specified  $K_j$  parameters satisfy the condition in (1), since the largest possible realization of demand at node  $j$  is  $1.3\hat{d}_j$ , according to our demand scenario generation scheme. Finally, to investigate the impact of the parameter  $\rho$  on the accessibility and equity metrics, we consider different values from the range [0.215, 1]; the value 0.215 corresponds to  $\rho^*$  in (18).

## 6.2. Computational Results: Performance of the Hybrid Model

As discussed in §4.2, alternative allocation policies have different implications on equity and accessibility metrics. In this section, we aim to provide quantitative insights about the related trade-off between the accessibility and equity metrics, and perform a numerical analysis to illustrate the comparative performance of the hybrid model and its two special cases. In addition to these three models featuring different equitable supply allocation policies, we also consider a benchmark model (referred to as Model\_Base) which ignores the equity in supply allocation and only focuses on the accessibility.

*Equity performance.* To evaluate the performance of the models in terms of equity in supply distribution, in addition to the MPUD, we consider the average proportion of unsatisfied demand (APUD) across PODs. We construct the empirical cumulative distribution functions (CDFs) of the random APUD and MPUD; Figure 3 shows the corresponding CDFs for a

particular problem instance of each model. The solution of the hybrid model for this problem instance is partly shown in Figure 3 in the online supplement (Appendix C); in particular, we illustrate the opened PODs and the assignments of the demand points to the PODs under two representative scenarios.

In accordance with Proposition 4.2, Figure 3(a) illustrates that Model\_PD always performs better than all other models in terms of MPUD. Observe that the CDFs of APUD and MPUD are the same for Model\_PD (follows from (21)). According to Figure 3(b), Model\_PD also performs generally better in terms of APUD (even though there does not exist a stochastic dominance relation in terms of APUD). Additionally, we observe that Model\_Hybrid performs generally better than Model\_TD in terms of both PUD metrics. More interestingly, the performance gap between Model\_Hybrid and Model\_PD is smaller in terms of APUD compared to MPUD.

*Accessibility performance.* Table 1 presents the values of accessibility metrics attained by each model under different parameter settings. Recall that SLM-RND maximizes the ETA (i.e., metric (I + II) in the table), where the metric (I) denotes the expected total accessibility of the PODs from the LDC and the metric (II) represents the expected total accessibility of the PODs from the demand locations. In these instances, we set  $\rho = 0.3$  and vary the values of the parameters  $\tau$  and  $c$ . Because Model\_TD and Model\_Hybrid achieve the same level of accessibility by design, only the results of the latter model are presented in the table.

According to the results in Table 1, Model\_PD can significantly compromise from accessibility, whereas the performance of Model\_Hybrid in terms of accessibility is very similar to that of Model\_Base. The average relative decrease in ETA by Model\_PD with respect to Model\_Hybrid is 4.2%, and it is even larger (12.3%) for the expected total accessibility of the PODs from the demand locations (i.e., metric II). On the other hand, the average relative decrease in ETA by Model\_Hybrid with respect to Model\_Base is only 1.1%. We can also see from Table 1 that the trade-off between accessibility and equity in supply distribution for Model\_PD and Model\_Hybrid becomes more significant for small values of  $c$ . For instance, for  $c = 1.5$  and  $\tau = 0.02$ , the average relative differences between Model\_PD and Model\_Hybrid are 25.3% and 42.6% in terms of the metrics I + II and II, respectively. Similarly, for  $c = 1.3$  and  $\tau = 0.01$ , Model\_Hybrid performs 4.8% and 22.9% better than Model\_PD on average. These results are expected because less accessible PODs often have to be selected in the presence of strong capacity limitations. The restrictive PD policy can even lead to infeasible formulations. The results are also consistent with Observation 4.1 in §4, which

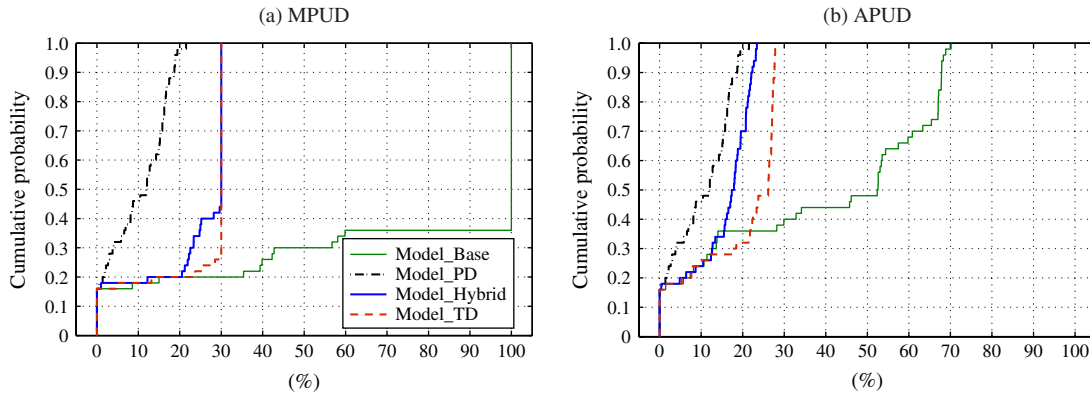


**Figure 3** (Color online) Empirical Cumulative Distribution Functions of MPUD and APUD ( $\tau = 0.03, c = 2.5, \rho = 0.3$ )

analytically shows that Model\_PD and Model\_Hybrid attain the same objective function value for sufficiently large  $K_j$  values. Finally, as observed from Table 1, for a fixed value of the capacity parameter  $c$ ,

the ETA associated with a given model decreases as  $\tau$  increases; this highlights the role of  $\tau$  in balancing the trade-off between equity and efficiency in accessibility (as discussed in §4.1).

**Table 1** Accessibility Statistics for Model\_Base, Model\_PD, and Model\_Hybrid Under Different  $\tau$  and  $c$  ( $\rho = 0.3$  and  $|S| = 50$ )

Parameters	Model	Accessibility metrics			Relative decreases (%) <sup>a</sup>		
		(I)	(II)	(I+II)	(I)	(II)	(I+II)
$\tau = 0.03$ $c = 2.0$	Model_Base	3.6416	3.7371	7.3787			
	Model_PD <sup>b</sup>	—	—	—			
$\tau = 0.03$ $c = 2.5$	Model_Hybrid	3.6416	3.7211	7.3627	0.0	0.4	0.2
	Model_PD	3.7233	3.7577	7.4810	0.1	0.9	0.5
$\tau = 0.02$ $c = 1.3$	Model_Hybrid	3.6416	3.7734	7.4150	2.1	-1.3	0.4
	Model_Base	3.6453	3.8069	7.4521			
$\tau = 0.02$ $c = 1.5$	Model_PD <sup>b</sup>	3.5456	3.4426	6.9882			
	Model_Hybrid	3.5456	3.1138	6.6594	0.0	9.6	4.7
$\tau = 0.02$ $c = 2.0$	Model_Hybrid	3.5456	3.5387	7.0843	8.8	42.6	25.3
	Model_Base	3.2333	1.9356	5.1690	0.0	4.7	2.3
$\tau = 0.02$ $c = 2.5$	Model_Hybrid	3.5456	3.3731	6.9187			
	Model_Base	3.4869	3.5519	7.8425	0.0	3.8	1.7
$\tau = 0.01$ $c = 1.3$	Model_Hybrid	3.4869	3.3876	7.6745	0.1	0.9	0.4
	Model_Base	4.2906	4.2869	7.8076	0.1		
$\tau = 0.01$ $c = 1.5$	Model_Hybrid	4.4850	3.5214	8.1211	0.1	1.9	0.9
	Model_Base	4.4813	3.5507	8.0319	0.0	0.5	0.2
$\tau = 0.01$ $c = 2.0$	Model_Hybrid	4.4850	3.6196	8.1045	0.0		
	Model_Base	4.4850	4.9182	8.4397	0.1	1.9	0.9
$\tau = 0.01$ $c = 2.5$	Model_Hybrid	4.4813	5.2645	7.8187	-7.4	22.9	4.8
	Model_Base	4.4850	4.8999	8.2146	0.4	5.9	2.7
$\tau = 0.01$ $c = 1.5$	Model_Hybrid	4.4850	4.9182	8.5215			
	Model_Base	4.8999	4.8999	8.1829	-1.1	7.4	2.5
$\tau = 0.01$ $c = 2.0$	Model_Hybrid	4.8999	4.8485	8.3940	1.4	1.6	1.5
	Model_Base	4.8999	4.9182	8.6199			
$\tau = 0.01$ $c = 2.5$	Model_Hybrid	4.8999	4.8485	8.5686	0.0	1.6	0.7
	Model_Base	4.8999	4.8485	8.5077	1.4	-0.5	0.6
	Model_Hybrid	4.8999	4.8485	8.5686			
	Average for Model_PD	4.8485	4.8485	8.5848	-5.9	7.3	0.3
	Average for Model_Hybrid	4.8485	4.5785	8.6082	6.9	-7.8	0.6
					-2.9	12.3	4.2
					1.5	0.5	1.1

<sup>a</sup>The relative decreases are computed with respect to Model\_Base (◊) or Model\_Hybrid (△).

<sup>b</sup>No feasible solution.

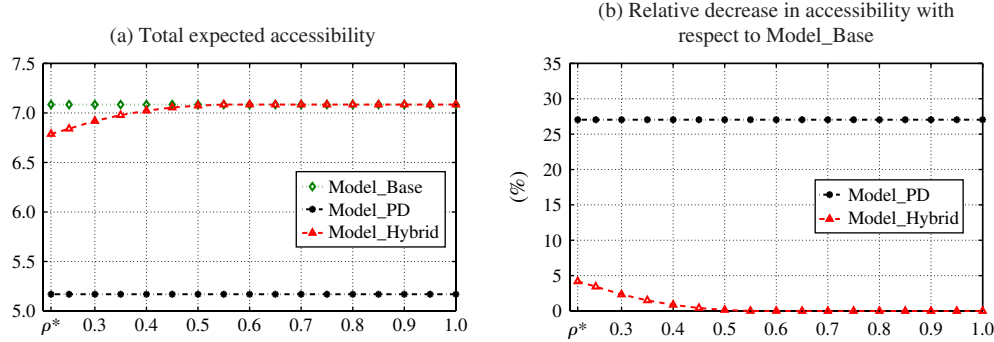


**Figure 4** (Color online) Accessibility with Respect to  $\rho$  ( $\tau = 0.02, c = 1.5$ )

*Effects of  $\rho$  on accessibility and equity.* We also study the effects of the parameter  $\rho$  on the accessibility and the PUD metrics. Recall that  $\rho$  represents an upper bound on the unsatisfied demand ratio for each POD and scenario. Figure 4(a) presents the ETA associated with the alternative models for different values of  $\rho$ , and Figure 4(b) shows the relative decrease in ETA with respect to Model\_Base. To evaluate the models in terms of the PUD, we present the maximum (over the scenarios) and the expected APUD and MPUD values for different  $\rho$  values in Figures 5 and 6, respectively.

According to Figures 4(a) and 4(b), the relative difference between Model\_Hybrid (and Model\_TD) and Model\_Base in terms of ETA decreases and converges to zero with increasing  $\rho$ , as expected. Similarly, as the parameter  $\rho$  increases, the performance of Model\_Hybrid (and Model\_TD) becomes closer to that of Model\_Base and moves away from that of Model\_PD in terms of equity. According to Figure 5, when  $\rho$  equals  $\rho^* = 0.215$ , Model\_Hybrid (and Model\_TD) leads to the same values of the maximum MPUD and APUD as Model\_PD. As  $\rho$  increases, the maximum MPUD and APUD provided by Model\_TD and Model\_Hybrid initially move away from those provided by Model\_PD. As we continue to increase  $\rho$ , the maximum MPUD and APUD associated with Model\_Hybrid eventually stabilize, and the values of these metrics for Model\_TD continue to increase (as expected, perfectly linear with slope 1 for the maximum MPUD), and get close to those of Model\_Base. This is because Model\_Hybrid always gets as close as possible to the solution of Model\_PD in terms of the supply distribution, whereas Model\_TD gives less importance to equity as  $\rho$  increases. Indeed, when  $\rho$  is sufficiently large, Model\_TD becomes Model\_Base and Model\_Hybrid corresponds to a special case that involves only the relaxed PD policy.

According to Figure 6, the trends in the relative performances of models with respect to the expected APUD and MPUD are similar to those in terms of the maximum APUD and MPUD. However, as seen from Figure 6, even if we set  $\rho = \rho^*$ , the expected APUD and MPUD provided by Model\_TD

and Model\_Hybrid do not reach the 10% level provided by Model\_PD. This follows from the fact that setting  $\rho = \rho^*$  in Model\_TD and Model\_Hybrid is not sufficient to ensure the proportional distribution of supplies, as discussed in §4.2.

In summary, the numerical results in this section confirm the competitive performance of the Model\_Hybrid both in terms of the accessibility and equity. Moreover, we show that the values of input parameters (including upper bounds on the POD capacities, accessibility threshold, and minimum shortage ratio) can significantly affect both the model performance and the trade-off between the accessibility and equity metrics.

### 6.3. Computational Results: Performance of the Proposed Algorithm

To assess the effectiveness of the proposed integer L-shaped algorithm, we conduct a computational study on instances with  $|I| = 30, 60, 94$ , and  $|S| = 50, 100, 200, 500$ . For each choice of  $|I|$ , we determine a set of low, medium, and high values for the  $\tau$  and  $c$  parameters, following the scheme presented in §6.1. To avoid easy-to-solve cases, we neglect the combinations of parameters that involve the high values of  $c$  with the low and medium values of  $\tau$ , and the low values of  $c$  with the high values of  $\tau$ .

We benchmark our algorithm against the state-of-the-art mixed-integer solver CPLEX. All of the MILP formulations were solved by CPLEX 12.5.0.1 using the absolute and relative optimality gaps of  $10^{-6}$  and  $10^{-4}$  as the stopping criteria, respectively. The IntLS algorithm was implemented in C++ using the Concert Technology component library of CPLEX 12.5.0.1, and the Boost C++ Libraries (Version 1.54.0) were used for parallel computing. The tests were carried out on an HP workstation with two Intel Xeon W5580 3.2 GHz and 32 GB RAM running on Microsoft Windows Server 2003 R2 Enterprise x64 Edition. We use a maximum of eight concurrent threads and set a time limit of 7,200 seconds.

It is well known that solving the large-scaled DEFs using a standard mixed-integer programming solver

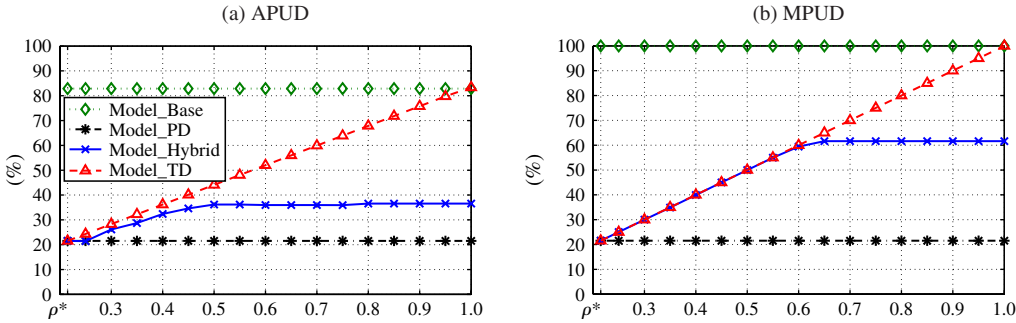


Figure 5 (Color online) Maximum APUD and MPUD with Respect to  $\rho$  ( $\tau = 0.02, c = 1.5$ )

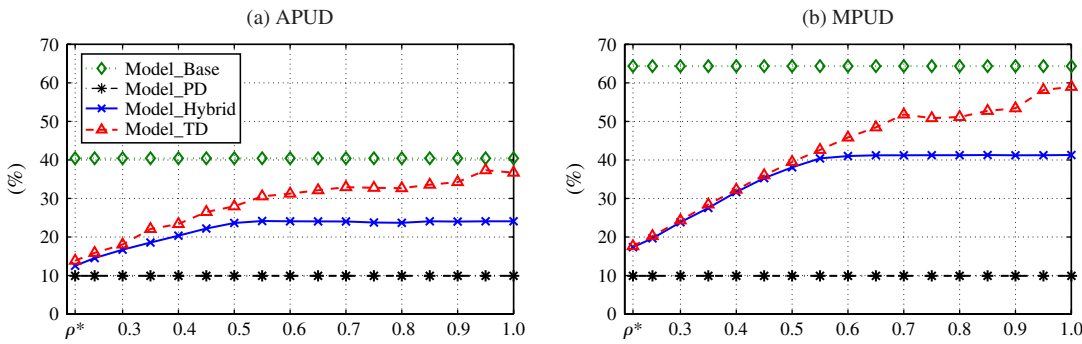


Figure 6 (Color online) Expected APUD and MPUD with Respect to  $\rho$  ( $\tau = 0.02, c = 1.5$ )

is generally hard for large problem instances. In our experiment, CPLEX could not provide optimal solutions within the prescribed time limit for most of the large problem instances. For such cases, we record both the best upper bound on the optimal objective value (retrieved from CPLEX and denoted by  $\overline{\text{Obf}}$ ) and the best available objective value within the time limit (denoted by  $\text{Obf}^*$ ). Then, we calculate an upper bound on the relative optimality gap as follows:

$$\text{UBROG} = \frac{\overline{\text{Obf}} - \text{Obf}^*}{\text{Obf}^*}.$$

The results related to the computational performances of *IntLS* and CPLEX are presented in Table 2; all of the results are averaged over three instances. In particular, this table presents the elapsed solution times, the UBROG values that are larger than 1%, and the relative reduction in the elapsed solution times by *IntLS* with respect to CPLEX. We observe that CPLEX could not even provide any feasible solution for a large number of the instances. For these instances, we use the best available lower bound on the optimal objective value to calculate an upper bound on the optimality gap; these upper bounds turn out to be extremely high when the number of demand points and scenarios is large. In contrast to CPLEX, *IntLS* obtained an optimal solution for the majority of the instances in significantly shorter times. As seen in Table 2, the relative reduction in solution times by

*IntLS* can reach up to 99.7%. These improvements in solution times generally grow with the increasing numbers of demand points and scenarios. For very difficult instances, such as the ones with  $|I| = 60$  and  $|S| = 200$ , the relative reduction in solution times appears to be relatively small; however, this is mainly due to the fact that the maximum time limit is kept fixed independent of the complexity of the instances. The results also indicate that the computational performance is significantly affected by the parameter  $\tau$ , regardless of the solution algorithm used. This is because the higher values of  $\tau$  result in smaller coverage sets, and consequently, smaller feasible regions. We also observe that the effect of  $\tau$  typically becomes more evident with the increasing number of demand points and scenarios.

In summary, the computational study illustrates that the performance of *IntLS* is significantly better compared with that of CPLEX and we can solve the proposed model for reasonably large numbers of nodes and scenarios.

## 7. Conclusion

In this study, we introduce the stochastic last mile distribution network design problem, which determines the locations and capacities of PODs while considering the demand- and network-related uncertainties in the post-disaster environment. We characterize the concepts of accessibility and equity in

**Table 2** Elapsed Solution Times, the UBROG Values (%), and the Relative Reduction in Solution Times with Respect to CPLEX (%),  $\rho = 0.3$

$ I $	$(\tau, c)$	$ S  = 50$			$ S  = 100$			$ S  = 200$			$ S  = 500$		
		$IntL\mathcal{S}$		CPLEX	$IntL\mathcal{S}$		CPLEX	$IntL\mathcal{S}$		CPLEX	$IntL\mathcal{S}$		CPLEX
		Rel. Reduc.	Rel. Reduc.	Rel. Reduc.	Rel. Reduc.	Rel. Reduc.	Rel. Reduc.	Rel. Reduc.	Rel. Reduc.	Rel. Reduc.	Rel. Reduc.	Rel. Reduc.	Rel. Reduc.
30	(0.01, 1.5) (0.01, 2.0) (0.02, 1.5) (0.02, 2.0) (0.03, 2.25) (0.03, 2.75)	17 18 9 9 2 2	25 51 43.1 28.6 9 9	29.5 37.2 16 14 79.0 71.8	37 36 16 14 4 4	278 113 66 73 32 39	81.6 62.4 75.0 79.6 85.8 87.5	98 81 16 37 8 8	1,018 329 610 477 235 293	87.5 75.3 96.9 89.1 96.1 95.0	234 176 18 81 24 24	4,835 4,646 4,067 [218] 4,148 [568] 2,041 1,136	94.9 95.6 >99.2 >96.9 98.7 96.7
60	(0.05, 2.5) (0.05, 3.0) (0.065, 2.5) (0.065, 2.5) (0.065, 3.0) (0.08, 3.25) (0.08, 3.75)	224 150 29 393 39 773 7	5,092†† 5,656† 97.3 292 92.5 93.7 98.1	>89.7 >97.3 292 7,210 61 91 14	487 282 7,202 [878]** 2,356 2,856 5,066††	>93.2 >96.0 >96.0 804 209 174 >99.4	989 7,203 [1,268]*** [1,315]*** 96.4 96.1 16	7,203 7,202 [1,315]*** [1,329]*** 209 7,205 6,605	>86.3 >88.8 >88.8 5,169 [2]† 380 1,007 >99.7	4,689 7,205 5,169 [2]† 7,206 [1,329]*** 7,205 7,205 54	7,205 7,205 28.3 >94.7 86.0 >99.2 7,205 7,205 >99.2		
94	(0.08, 3.5) (0.08, 4.0) (0.10, 3.5) (0.10, 4.0) (0.12, 4.25) (0.12, 4.75)	585 408 292 290 81 77	1,904 1,363 2,095 1,791 1,256 1,703	48.8 66.9 84.9 80.5 92.9 92.5	1,528 826 674 875 92.9 92.5	6,092 5,615 6,609 6,179 5,977 4,403	[▲]† [▲] [▲]** [▲]** [888]† 156	>72.7 >85.8 >89.6 >85.4 >97.7 96.3	2,535 2,170 1,467 2,088 222 220	7,206 7,207 7,205 7,207 7,205 7,205	>64.8 >69.9 >79.6 >71.0 >96.9 88.5	5,835 [3]† 6,145 [2]†† 6,102 [5]†† 7,175 [2]†† 608 —	

Notes: UBROG values are reported in [ ]; the values above 5,000% are indicated with ▲ and the values below 1% are not reported.

†Time limit with integer feasible solution (for example, †† represents two such instances).

\* Time limit with no integer feasible solution (for example, \*\*\* represents three such instances).

—, Out of memory.

the context of last mile distribution network design and provide performance metrics to incorporate these concerns into mathematical programming models. We develop a two-stage stochastic programming model that can achieve high levels of accessibility and equity simultaneously. Finally, we devise a Benders decomposition-based branch-and-cut algorithm to solve large problem instances. Computational experiments illustrate the value of the proposed model and show that the algorithm can attain optimal solutions in significantly shorter times compared to CPLEX.

There are several areas that future work can focus on. One avenue of extension to this work is to also consider the decisions on the numbers and locations of LDCs. If some LDCs with prepositioned supplies already exist in the network, then these supplies might also have to be moved to new LDCs to improve accessibility. As part of our ongoing research, we are addressing the design of such multiechelon last mile networks, where logistical costs associated with supply reallocation are also important. Future work can also focus on developing risk-averse versions of the proposed model.

## Supplemental Material

Supplemental material to this paper is available at <http://dx.doi.org/10.1287/trsc.2015.0621>.

## Acknowledgments

The authors thank Ceyda Sol from Sabancı University for her valuable help with the data collection process and making some figures. The authors also thank the anonymous referees and the associate editor for their valuable comments and suggestions. The authors have been supported by the Scientific and Technological Research Council of Turkey (TUBITAK) Career Award [111M543]. The first and second authors also acknowledge the support from Bilim Akademisi—The Science Academy, Turkey, under the BAGEP program.

## References

- Afshar A, Haghani A (2012) Modeling integrated supply chain logistics in real-time large-scale disaster relief operations. *Socio-Econom. Planning Sci.* 46(4):327–338.
- Ahmed S (2006) Convexity and decomposition of mean-risk stochastic programs. *Math. Programming* 106(3):433–446.
- Avci İ (2011) Officials, locals highlight problems with distribution relief packages. *Today's Zaman* (October 26). Accessed July 17, 2013, <http://www.todayszaman.com/news-261058-officials-locals-highlight-problems-with-distribution-of-relief-packages.html>.
- Balcık B, Beamon BM, Smilowitz K (2008) Last mile distribution for humanitarian relief chains. *J. Intelligent Transportation Systems* 12(2):51–63.
- Barbarosoglu G, Arda Y (2004) A two-stage stochastic programming framework for transportation planning in disaster response. *J. Oper. Res. Soc.* 55(1):43–53.
- Barth D (2009) The bright side of sitting in traffic: Crowdsourcing road congestion data (August 25). Accessed July 17, 2013, <http://googleblog.blogspot.com/2009/08/bright-side-of-sitting-in-traffic.html#!/2009/08/bright-side-of-sitting-in-traffic.html>.
- Birge JR, Louveaux FV (1997) *Introduction to Stochastic Programming* (Springer, New York).
- Campbell AM, Vandenbussche D, Hermann W (2008) Routing for relief efforts. *Transportation Sci.* 42(2):127–145.
- Erdik M, Eren K (1983) Attenuation of intensities for earthquake associated with the North Anatolian Fault. Technical report, Middle East Technical University Earthquake Engineering Research Center, Ankara, Turkey.
- Felder S, Brinkmann H (2002) Spatial allocation of emergency medical services: Minimizing the death rate of providing equal access? *Regional Sci. Urban Econom.* 32(1):27–45.
- Horner M, Downs J (2007) A flexible GIS-based network flow model for routing hurricane disaster relief goods. *Transportation Res. Record* 2022:47–54.
- Horner M, Downs J (2008) Analysis of effects of socioeconomic status on hurricane disaster relief plans. *Transportation Res. Record* 2067:1–10.
- Horner M, Downs J (2010) Optimizing hurricane disaster relief goods distribution: Model development and application with respect to planning strategies. *Disasters* 34(3):821–844.
- Horner M, Widener M (2011) The effects of transportation network failure on people's accessibility to hurricane disaster relief goods: a modeling approach and application to a Florida case study. *Natural Hazards* 59(3):1619–1634.
- Huang M, Smilowitz K, Balçık B (2012) Models for relief routing: Equity, efficiency and efficacy. *Transportation Res. Part E: Logist. Transportation Rev.* 48(1):2–18.
- IBM ILOG CPLEX (2013) *IBM ILOG CPLEX Optimization Studio 12.5 Information Center*. Accessed June 26, 2013, <http://pic.dhe.ibm.com/infocenter/cosinfoc/v12r5/index.jsp>.
- IFRC (2012) Emergency appeal operation update; Turkey: Van earthquake, International Federation of Red Cross and Red Crescent Societies (IFRC). Technical report. Accessed October 2, 2014, <http://adore.ifrc.org/Download.aspx?FieldId=26250>.
- IFRC (2013) Disaster relief emergency fund (DREF). Ghana: Floods, International Federation of Red Cross and Red Crescent Societies (IFRC). Technical report. Accessed May 17, 2013, <http://reliefweb.int/sites/reliefweb.int/files/resources/MDRGH009.pdf>.
- Klein Haneveld WK, van der Vlerk MH (1999) Stochastic integer programming: General models and algorithms. *Ann. Oper. Res.* 85:39–57.
- Kovacs G, Spens K (2007) Humanitarian logistics in disaster relief operations. *Internat. J. Physical Distribution Logist. Management* 37(2):99–114.
- Kovacs G, Tatham P (2009) Humanitarian logistics performance in the light of gender. *Internat. J. Productivity Performance Management* 58(2):174–187.
- Laporte G, Louveaux FV (1993) The integer L-shaped method for stochastic integer programs with complete recourse. *Oper. Res. Lett.* 13(3):133–142.
- Lin YH, Batta R, Rogerson PA, Blatt A, Flanigan M (2012) Location of temporary depots to facilitate relief operations after an earthquake. *Socio-Econom. Planning Sci.* 46(2):112–123.
- Marsh M, Schilling D (1994) Equity measurement in facility location analysis: A review and framework. *Eur. J. Oper. Res.* 74(1):1–17.
- McCoy J, Lee H (2014) Using fairness models to improve equity in health delivery fleet management. *Production Oper. Management* 23(6):965–977.
- Morrow B (1999) Identifying and mapping community vulnerability. *Disasters* 23(1):1–18.
- Müller A, Stoyan D (2002) *Comparison Methods for Stochastic Models and Risks* (John Wiley and Sons, Chichester, UK).
- Mulligan G (1991) Equality measures and facility location. *Papers Regional Sci.* 70(4):345–365.
- Noyan N (2010) Alternate risk measures for emergency medical service system design. *Ann. Oper. Res.* 181(1):559–589.

- Noyan N (2012) Risk-averse two-stage stochastic programming with an application to disaster management. *Comput. Oper. Res.* 39(3):541–559.
- Ntiamo L, Sen S (2008) A comparative study of decomposition algorithms for stochastic combinatorial optimization. *Comput. Optim. Appl.* 40(3):299–319.
- OCHA (2013) Office for the Coordination of Humanitarian Affairs (OCHA) South Sudan weekly humanitarian bulletin for the period 16–22 July 2012. Accessed May 17, 2013, <http://www.sudantribune.com/spip.php?article43404>.
- Rath S, Gutjahr W (2011) A math-heuristic for the warehouse location-routing problem in disaster relief. *Comput. Oper. Res.* 42:25–39.
- Rubin P (2011) Benders decomposition then and now. Accessed June 29, 2013, <http://orinanobworld.blogspot.com/2011/10/benders-decomposition-then-and-now.html>.
- Sen H, Bulbul K (2015) A strong preemptive relaxation for weighted tardiness and earliness/tardiness problems on unrelated parallel machines. *INFORMS J. Comput.* 27(1):135–150.
- Sen S (2005) Algorithms for stochastic mixed-integer programming models. Aardal K, Nemhauser G, Weismantel R, eds. *Discrete Optimization*, Handbooks Oper. Res. Management Sci., Vol. 12 (Elsevier, Amsterdam), 515–558.
- Sen S, Higle JL (2005) The  $C^3$  theorem and a  $D^2$  algorithm for large scale stochastic mixed-integer programming: Set convexification. *Math. Programming* 104(1):1–20.
- Sphere Project (2011) Sphere project: Humanitarian charter and minimum standards in humanitarian response. Technical report, Geneva. Accessed August 30, 2013, <http://www.sphereproject.org/resources/?search=1&keywords=&language=English&category=22&subcat-22=23&subcat-29=0&subcat-31=0&subcat-35=0&subcat-49=0>.
- Stephenson R (1993) *Disaster Management Training Programme, Logistics Guide Module* (United Nations Development Program, New York), 12–13.
- Tricoire F, Graf A, Gutjahr W (2012) The bi-objective stochastic covering tour problem. *Comput. Oper. Res.* 39(7):1582–1592.
- Turkish Statistical Institute (TUIK) (2012) Accessed August 31, 2013, <http://tuikapp.tuik.gov.tr/adnksdagitapp/adnks.zul>.
- Tzeng G, Cheng H, Huang T (2007) Multi-objective optimal planning for designing relief delivery systems. *Transportation Res. Part E: Logist. Transportation Rev.* 43(6):673–686.
- Van Slyke RM, Wets R (1969) L-shaped linear programs with applications to optimal control and stochastic programming. *SIAM J. Appl. Math.* 17(4):638–663.
- Vitoriano B, Ortuno MT, Tirado G, Montero J (2011) A multi-criteria optimization model for humanitarian aid distribution. *J. Global Optim.* 51(2):189–208.
- Widener M, Horner M (2011) A hierarchical approach to modeling hurricane disaster relief goods distribution. *J. Transport Geography* 19(4):821–828.
- Yi W, Ozdamar L (2007) A dynamic logistics coordination model for evacuation and support in disaster response activities. *Eur. J. Oper. Res.* 179(3):1177–1193.
- Yuan Y, Sen S (2009) Enhanced cut generation methods for decomposition-based branch and cut for two-stage stochastic mixed-integer programs. *INFORMS J. Comput.* 21(3): 480–487.
- Zakour M, Harrell E (2004) Access to disaster services. *J. Soc. Service Res.* 30(2):27–54.
- Ziflioğlu V (2011) Problems in distribution shade aid efforts in Van. *Hürriyet Daily News* (September 23). Accessed July 17, 2013, <http://www.hurriyedailynews.com/default.aspx?pageid=438&=problems-in-distribution-shade-aid-efforts-in-van-2011-10-25>.